CEG1 DEPLETION REVEALS MECHANISMS GOVERNING DEGRADATION OF NON-CAPPED RNAs

Onofrio Zanin[1], Daniel Hebenstreit[2] and Pawel Grzechnik[3*]

[1]School of Biosciences, University of Birmingham, Edgbaston, Birmingham, B15 2TT, UK

[2]School of Life Sciences, University of Warwick, Coventry CV4 7AL, UK

[3]School of Biological Sciences, University of Manchester, Oxford Road, Manchester M13 9PT, UK

*Correspondence: pawel.grzechnik@manchester.ac.uk

ABSTRACT

Most functional eukaryotic mRNAs contain a 7-methylguanosine (m7G) cap which serves as a platform that recruits proteins to support essential biological functions such as mRNA processing, nuclear export and translation. Although capping is accomplished during the first steps of transcription the fate and turnover of uncapped transcripts have not been studied extensively. Here, we employed fast nuclear depletion of the capping enzymes in *Saccharomyces cerevisiae* to uncover the turnover of the transcripts that failed to be capped. We show that the levels of non-capped mRNAs are determined principally by the abundance of their synthesis. Nuclear depletion of the capping enzymes increases the levels of lowly expressed mRNAs and decreases mRNAs that are highly transcribed altogether mimicking the effects observed in cells lacking the predominantly cytoplasmic 5'-3' exonuclease Xrn1. The nuclear 5'-3' exonuclease Rat1 is not involved in the degradation of cap-defective transcripts and the lack of the capping does not affect the distribution of RNA Polymerase II on the chromatin. Our data indicate that the mRNAs that failed to be capped are not directed to a specific quality-control pathway and that the 5' cap role is associated with the Xrn1-dependent buffering of the cellular mRNA levels, along with protecting from 5'-3' degradation.

Key words: capping / RNA degradation / transcription

51 **INTRODUCTION**

52 The N7-methylated guanosine (m7G cap) linked to the first nucleotide of the RNA
53 molecule, is a hallmark structure of eukaryotic transcripts generated by the RNA
54 Polymerase II (Pol II). The cap is involved in various steps of mRNA turnover,
55 processing, transport and translation and therefore, essential for cell viability (Schwer,
56 Mao and Shuman, 1998; Furuichi, 2015). Many of these biological functions are
57 related to the cap-binding complex (CBC) which binds to the m7G caps of nascent
58 RNAs (Izaurralde et al., 1995; Izaurralde et al., 1994).

59 The biosynthesis of the m7G cap requires three enzymes: the RNA triphosphatase
60 (TPase) which removes the γ-phosphate from the RNA 5′ end; the RNA
61 guanylyltransferase (GTase) which transfers a GMP group to the diphosphate 5′ end;
62 and the guanine-N7 methyltransferase adding a methyl group to the N7 amine of the
63 guanine cap (Decroly *et al.*, 2012). This synthesis pathway of the m7G cap is
64 conserved in eukaryotes, however, the enzymes involved vary between the organisms
65 (Ramanathan, Robb and Chan, 2016). In humans and other higher eukaryotes, a
66 bifunctional protein RNGTT acts as RNA guanylyltransferase and 5′-triphosphatase
67 while the methylation is mediated by a separate protein RNMT (Varshney *et al.*, 2018).
68 In *S. cerevisiae* there are three proteins responsible for the RNA capping: the
69 guanylyltransferase Ceg1 and the 5′-triphosphatase Cet1 work together as a stable
70 heterodimer or heterotetramer, while the methyltransferase Abd1 acts independently
71 (Schroeder *et al.*, 2000; Hausmann, Pei and Shuman, 2003; Martinez-Rucobo *et al.*,
72 2015). The capping enzymes are recruited to the Pol II at the early stage of
73 transcription. In *S. cerevisiae*, Cet1 and Ceg1 bind the serine 5 phosphorylated C-
74 terminal domain (CTD) of Pol II at the transcription start site (TSS) (Schroeder *et al.*,
75 2000; Lidschreiber, Leike and Cramer, 2013). When the nascent RNA reaches the

length of ~17 nt, the Ceg1-Cet1 complex docks to the Pol II surface close to the RNA exit tunnel (Martinez-Rucobo *et al.*, 2015) and adds the terminal guanosine as soon as the first 25–30 nt of the nascent transcript extrude from the transcribing complex (Shatkin and Manley, 2000). Changes in the phosphorylation status of the Pol II CTD promoting transcription elongation results in the rapid dissociation of Ceg1-Cet1 (Martinez-Rucobo *et al.*, 2015). This and the increased phosphorylation of CTD Ser2 promote the binding of Abd1, which is recruited about 110 nt downstream of the TSS (Lidschreiber, Leike and Cramer, 2013) and completes the formation of the m7G cap. If the methylation of the added 5' guanosine residue fails, the defective transcripts are detected by a surveillance mechanism that triggers decapping by Rai1 and subsequent RNA degradation by its co-factor, the 5'-3' exonuclease Rat1 (Jiao et al., 2010). The lack of the cap structure on the 5' end may also lead to co-transcriptional degradation of the nascent transcript. This process naturally occurs at the 3' ends of genes and is essential for transcription termination. The cleavage over the poly(A) signal in the RNA creates an unprotected 5' monophosphate RNA end in the nascent RNA. This serves as an entry point for Rat1 which co-transcriptionally degrades RNA pursuing the Pol II transcribing downstream of the gene (Kim *et al.*, 2004; West, Gromak and Proudfoot, 2004; Eaton *et al.*, 2020). If the degradation rate exceeds the RNA synthesis rate, Rat1 reaches the transcribing complex and Pol II is displaced from DNA (Cortazar et al., 2019; Eaton, Francis, Davidson, & West, 2020; Kim et al., 2004; West, Gromak, & Proudfoot, 2004). A similar mechanism has been suggested to be active upstream to the transcription end site (TES) when the capping fails at the 5' ends of the genes. Analysis of the *FMP27* gene in *S. cerevisiae* revealed that the transcription of uncapped pre-mRNA is prematurely terminated by Rat1 within the gene body (Jimeno-González 2010). Moreover, analysis of the temperature-sensitive

101 mutants revealed that the inactivation of Ceg1 affects the accumulation of heat-shock
102 induced *SSA1* and *SSA4* mRNAs. However, their levels were restored by the deletion
103 of the predominantly cytoplasmic 5'-3' exonuclease Xrn1 (Schwer, Mao and Shuman,
104 1998). Xrn1 mediates the global mRNA degradation and therefore, together with the
105 decapping factors, acts as a sensor of the cellular mRNA levels that controls and
106 regulates the homeostatic mRNA abundance (Braun et al., 2012; Sun et al., 2013).
107 Here, we investigated the consequences of defective capping on RNA abundance and
108 transcription. We took advantage of the yeast model where, in contrast to metazoans,
109 CBC is not essential (Fortes *et al.*, 1999) which presents a unique opportunity to
110 distinguish between the functions of m7G cap and CBC. We employed rapid nuclear
111 depletion of Ceg1 to investigate the global turnover of the non-capped mRNAs. We
112 found that the absence of the capping complex resulted in the differential expression
113 of cellular RNAs: the mRNA levels of highly expressed genes decreased while the
114 mRNAs of genes expressed at lower levels increased. The deletion of *XRN1* resulted
115 in a similar redistribution in the mRNA abundance which was not synergistically
116 affected by the nuclear depletion of Ceg1. Our data indicate that both, m7G cap and
117 Xrn1 act closely in the control of the mRNA abundance. The non-capped mRNA levels
118 were not rescued by the inactivation of Rat1 exonuclease and the disruption of the 5'
119 end capping had a minor effect on the distribution of the Pol II on the chromatin.
120 Overall, our data indicate that the non-capped mRNAs are not simply evenly degraded
121 and that the cap plays an important role in the Xrn1-dependent sensing and buffering
122 of mRNA levels.
123
124
125

126 **RESULTS**

127 **Differential expression of non-capped mRNAs**

128 The impact of defective capping on the RNA expression has never been studied
129 genome-wide before. In our experimental approach, we employed the anchor-away
130 (AA) system (Haruki, Nishikawa and Laemmli, 2008) to deplete the capping enzymes
131 from the nucleus and rapidly affect the formation of the cap. FRB tag fused with Cet1,
132 Ceg1 or Abd1 (*cet1-AA*, *ceg1-AA* and *abd1-AA* strains) in the presence of rapamycin
133 heterodimerizes with FKBP12 attached to the ribosomal protein Rpl13a, which is
134 exported to the cytoplasm during the ribosome biogenesis, and thus removes the
135 capping enzymes from the nucleus. Since rapamycin affects the TOR signalling
136 pathway (Hausch et al. 2013) the strain used for this system carries the *tor1-1* mutation
137 which permits normal growth on rapamycin (Haruki, Nishikawa and Laemmli, 2008).
138 The nuclear depletion of Cet1 and Ceg1 were lethal (Fig. 1A) indicating the efficacy of
139 the method as cap formation is essential for cell viability (Tsukamoto *et al.*, 1997; Chu
140 and Shatkin, 2008). The inactivation of Abd1 activity has been shown to be lethal
141 (Mao, Schwer and Shuman, 1996), however, the nuclear depletion of Abd1 had no
142 impact on cell survival and only slightly affected the abundance of *ADH1* mRNA (Fig.
143 S1A). This indicates that Abd1 may be still functional after the relocation to the
144 cytoplasm. The nuclear depletion of either Cbp20 or Cbp80 was viable, consistent with
145 the fact that the CBC is not essential in *S. cerevisiae* (Fig. 1A).

146 In our functional experiments, the same yeast culture was split into a medium
147 containing either DMSO or rapamycin representing the WT (DMSO) or the nuclear
148 depletion (Rap) condition (Fig. 1B). First, we confirmed that RNA capping was indeed
149 affected by the nuclear depletion of Ceg1 (Fig. 1C). We co-immunoprecipitated the
150 RNA isolated from the *ceg1-AA* strain growing on either DMSO or Rap with the anti-

151 m7G cap antibody (H-20). The amount of capped *ADH1* mRNA (normalised to human
152 *GAPDH* spike) was reduced by 80% in *ceg1-AA* (Rap) when compared to WT (control
153 cells grown on DMSO). The nuclear depletion of either Ceg1 or Cet1 (*ceg1-AA* or *cet1-*
154 *AA*) resulted in a similar decrease in the *ADH1* mRNA (Fig. 1D and Fig. S1B) and
155 therefore, in the subsequent analyses, we focused mainly on the effects of Ceg1
156 removal. We also confirmed that the nuclear depletion of CBC did not affect *ADH1*
157 mRNA (Fig. 1D and Fig. S1B).
158 Next, we performed a global analysis to investigate genome-wide the mRNA levels
159 after Ceg1 nuclear depletion. We depleted Ceg1 for 45 minutes (min) as this time was
160 sufficient to decrease the *ADH1* level (Fig. S1B, 1D). Our RNA-seq analysis identified
161 1205 mRNAs affected by the nuclear depletion of Ceg1 (displaying log2 fold change
162 < -1 and > 1) (Fig. 1E). 736 (61%) of these mRNAs decreased when compared to the
163 control (WT), reflecting the fraction of non-capped transcripts that were subjected to
164 degradation. Unexpectedly, the levels of 469 genes (39%) increased (Fig. 1E). Both
165 effects were on average similar to each other (log2 fold change -1.4 and +1.5,
166 respectively) (Fig. S1C). We also tested how the levels of the mRNAs changed over
167 time during the nuclear depletion of Ceg1 (Fig. 1F). We selected *ADH1*, *PYK2* and
168 *PMA1* genes whose levels decreased upon Ceg1 depletion in the RNA-seq data. RT-
169 qPCR analysis revealed that their mRNAs decreased even further after 90 min and
170 stabilised after 120 min. We also tested *PML39*, *STP2* and *CTA1* whose levels
171 increased upon Ceg1 depletion in the RNA-seq data. *PML39* and *STP2* mRNAs
172 peaked after 90 min, while the accumulation of *CTA1,* displayed a constant increase
173 through time.

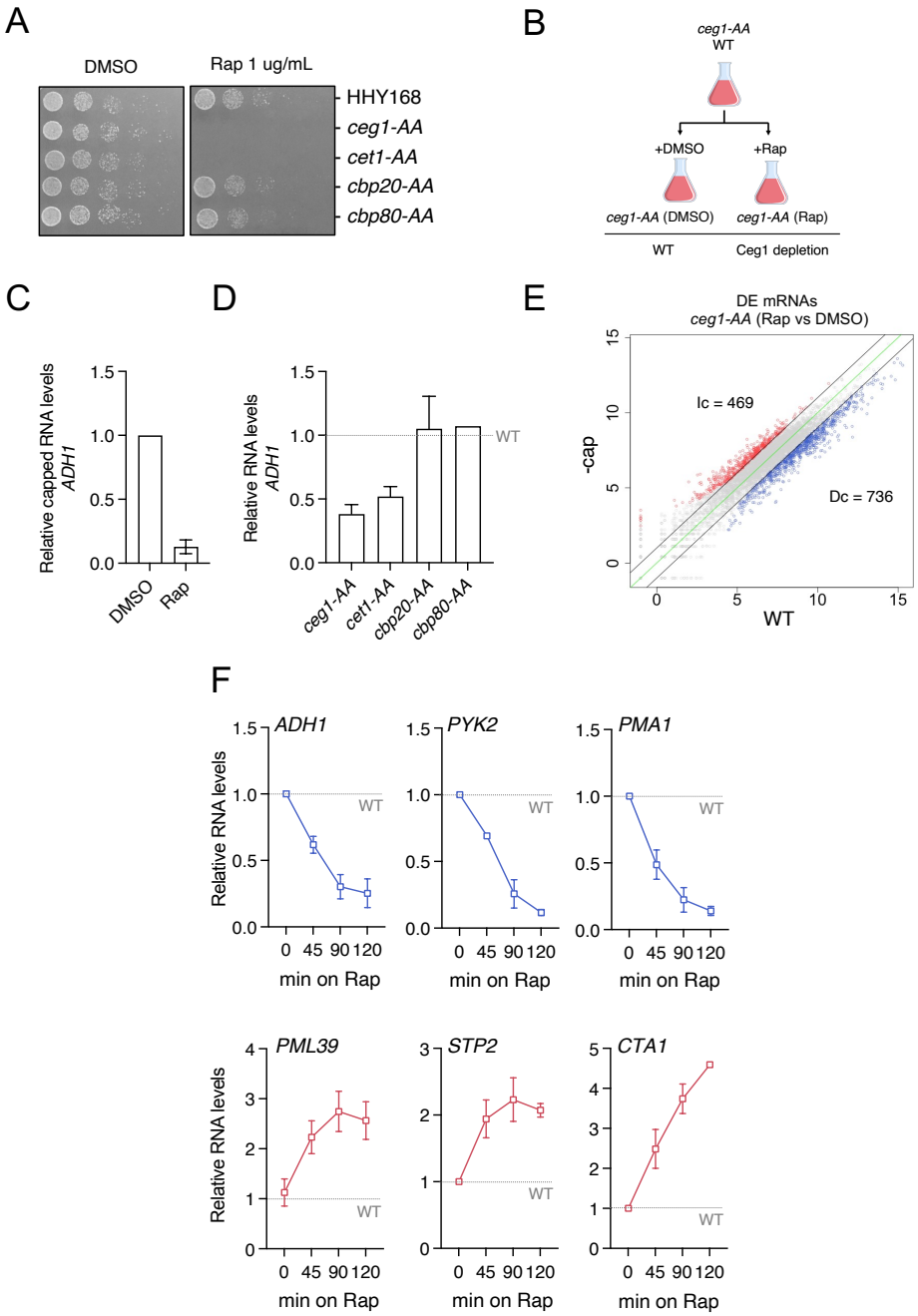

Figure 1. Nuclear depletion of capping enzymes results in differential accumulation of mRNAs. **A.** Spot test showing the growth of the AA strains. Serial dilution of each strain was spotted on solid YPD media in the presence of DMSO or rapamycin at the final concentration of 1 ug/mL. **B.** The outline of the experimental approach. Liquid cultures of cells at the exponential phase were split and supplemented with DMSO (control sample) or rapamycin (Rap; nuclear depletion sample) shown on the *ceg1-AA* example. **C.** Nuclear depletion of Ceg1 affects the formation of the m7G cap. Quantification of the capped RNA by RT-qPCR after 45 min of rapamycin treatment compared to control (DMSO). The RNA isolated from yeast was spiked-in with capped human RNA and immunoprecipitated by the anti-

183 m7G cap antibody (clone H20). The RNA levels were normalised to human *GAPDH* mRNA. The error
184 bars show standard deviation of three independent experiments. **D.** Nuclear depletion of the Cap
185 Binding Complex does not affect mRNA levels. RT-qPCR analysis of the *ADH1* mRNA levels after 45
186 min of rapamycin treatment compared to the control set to 1 (dotted line). The error bars show standard
187 deviation of two (*cbp20-AA* and *cbp80-AA*) or three independent experiments **E.** RNA-seq analysis
188 showing differential expression of mRNA species in *ceg1-AA* (Rap) strain (-cap) after 45 min of
189 rapamycin treatment compared to the control condition (WT). Increased (Ic) RNA species with log2 fold
190 change >1 are labelled in red. Decreased (Dc) RNA species showing log2 fold change <1 are in blue.
191 The zero-change line is in green and the ±1 log2 fold change threshold is indicated with continuous
192 black lines. **F.** The changes in mRNA levels over time during nuclear depletion of Ceg1. RT-qPCR
193 analysis of RNA levels for different genes measured at 0, 45, 90 and 120 min of rapamycin treatment
194 relative to control (WT) set to 1 (dotted line). The error bars show standard deviation of three
195 independent experiments.
196

197 **Accumulation of non-capped mRNAs depends on their expression level**

198 To understand the differential expression observed upon depletion of the capping
199 machinery we analysed the features of the affected mRNAs. First, we tested the basal
200 expression in WT cells (*ceg1-AA* on DMSO) for ~~the~~ differentially expressed mRNAs in
201 Ceg1-depleted cells. We found that increased mRNAs were generally lower
202 expressed (median transcript per million, log2 TPM = 2.7) than the decreased mRNAs
203 (median log2 TPM = 6.2) in WT (Fig. 2A). Next, we split all 1205 protein-coding genes
204 differentially expressed in *ceg1-AA* into three bins according to their expression levels
205 in WT cells: the top 25% were classified as highly expressed (High), the bottom 25%
206 as lowly expressed (Low) and the remaining 50% as medially expressed (Mid) (Fig.
207 2B). Most of the lowly expressed genes increased their mRNA levels (291 out of 301),
208 while most of the highly expressed mRNAs were decreased (300 out of 301) after the
209 Ceg1 depletion. Mid-range expressed genes were the least affected by the depletion;

210 however, they displayed the tendency to decrease the levels in Ceg1-depleted cells
211 (426 decreased versus 176 increased), correlating with increasing expression (Fig.
212 2B-C). Overall, we observed a progressive decrease of the log2 fold change for
213 mRNAs in *ceg1-AA* corelated with their increase in the basal expression levels in WT.
214 This was also reflected at the single gene level as shown for *ZRT1*, *STB4* and *ADH1*
215 (Fig. 2D). Next, we employed available datasets estimating mRNAs half-life (Geisberg
216 et al., 2015), transcription rates (TR) and Pol II density in *S. cerevisiae* (Pelechano,
217 Wei and Steinmetz, 2013) and applied them to the sets of differentially expressed
218 mRNAs identified in the *ceg1-AA*. These analyses revealed that the mRNAs which
219 increased upon Ceg1 nuclear depletion are more stable as they display longer half-
220 lives (average half-life 41.9 vs 30.7 min for decreased mRNAs) (Fig. 2E and S2A),
221 they also have lower transcription rates (Fig. 2F and S2B) and Pol II density (Fig. S2C)
222 than the genes whose mRNAs decreased in Ceg1-depleted cells. The mRNAs
223 accumulating in *ceg1-AA* were also longer than those from the decreased set (average
224 gene length 1430 vs 1113 nt) (Fig. S2D) consistently with the fact that shorter genes
225 are generally associated with higher expression (Urrutia and Hurst, 2003).
226 Interestingly, the MEME suite (https://meme-suite.org/meme/) analysis identified a
227 very pronounced sequence motif (A/G)GAAAA strongly enriched in the upregulated
228 mRNAs (Fig. 2G) however, its function remains unknown.
229 Gene ontology (GO) analysis showed that some mRNAs upregulated in *ceg1-AA* (45
230 out of the 469 tested) were associated with genes coding for DNA binding proteins
231 directly associated with transcription (Fig. S3A) including the zinc finger protein *PPR1,*
232 the regulator of stress response *STB5* and *PCF11,* a component of the 3' end
233 processing factor (Fig. S3B). GO terms analysis did not reveal consistent terms
234 emerging from the genes whose mRNAs decreased in Ceg1-depleted cells (Fig. S3C).

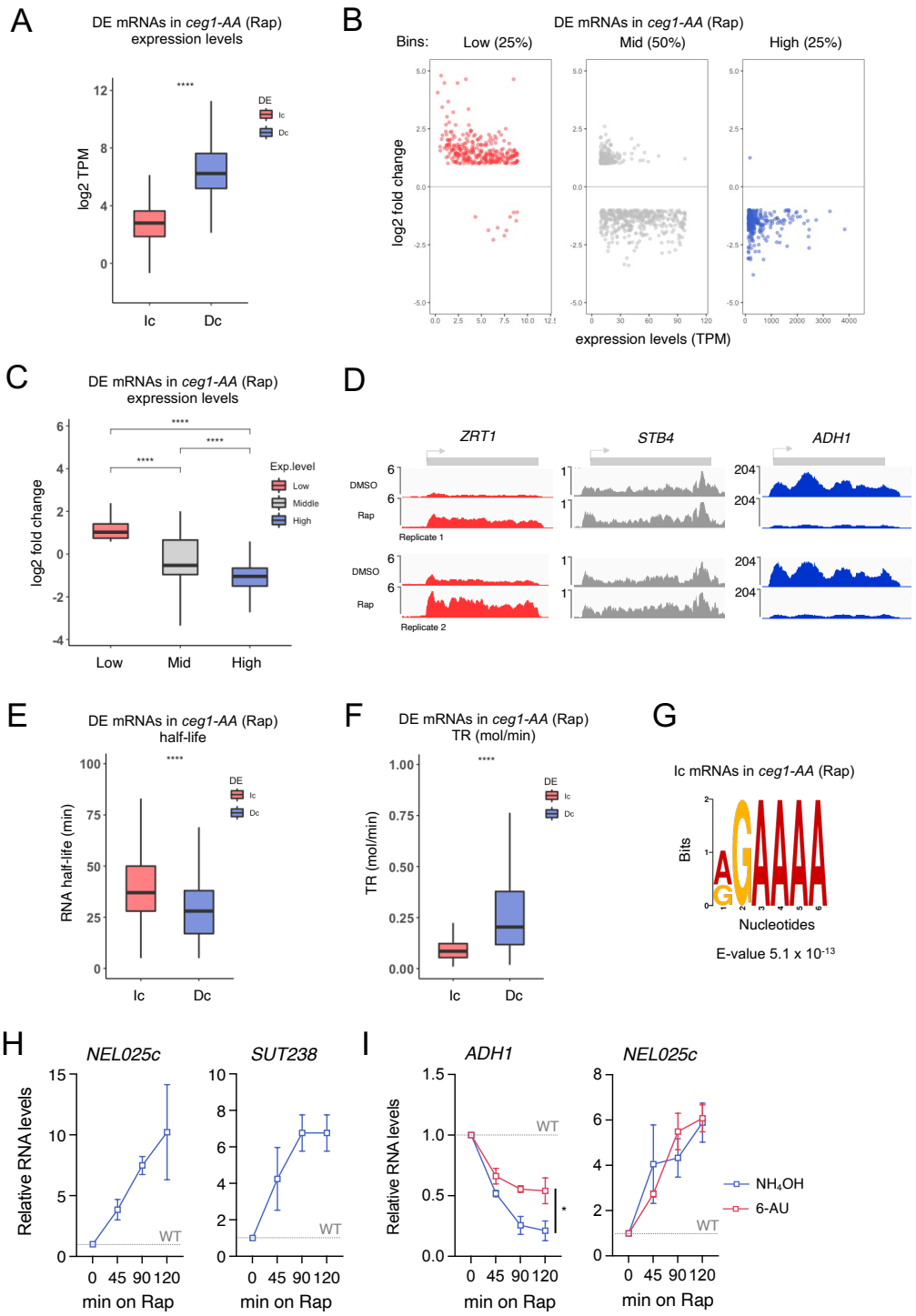

Figure 2. The accumulation of non-capped RNAs depend on gene expression levels

A. Differentially expressed mRNAs in *ceg1-AA* (Rap) vs *ceg1-AA* (DMSO/WT) sorted by their expression levels: Increased (Ic) or decreased (Dc). The expression levels were calculated by the log2 of Transcript Per Million (log2 TPM) value in WT (*ceg1-AA* on DMSO). **B.** The distribution of differentially expressed mRNAs in *ceg1-AA* (Rap) depending on their basal expression levels. **C.** The overall fold change for differentially expressed mRNAs in *ceg1-AA* (Rap) vs *ceg1-AA* (DMSO) ranked accordingly

242 to their basal expression levels. **D.** Genome viewer tracks showing RNA-seq reads in *ceg1-AA* (DMSO)
243 and *ceg1-AA* (Rap) for lowly (red), medial (grey) and highly (blue) expressed genes. **E-F.** Box plots
244 showing half-life (E) and transcription rates (F) of differentially expressed mRNAs in *ceg1-AA* (Rap) vs
245 *ceg1-AA* (DMSO). **G.** Logo sequence overrepresented in the increased mRNAs in *ceg1-AA* (Rap). **H.**
246 The accumulation of the *NEL025c* (left) and *SUT238* (right) RNAs in *ceg1-AA* strain upon 0, 45, 90 and
247 120 min of rapamycin treatment compared to WT set to 1 (dotted line). **I.** RT-qPCR analysis showing
248 the levels of *ADH1* mRNA and *NEL025* ncRNA upon 6-AU (red) and NH_4OH (blue) treatments in Ceg1-
249 depleted cells. The error bars show the standard deviation of three independent experiments. Statistical
250 analysis is shown for the last timepoint (120 min). **A, C, E, F.** ns=P > 0.05; *=P ≤ 0.05; **=P ≤ 0.01; ***=
251 P ≤ 0.001; ****= P ≤ 0.0001.
252
253 We also investigated Pol II-transcribed non-coding RNAs (ncRNAs), called cryptic
254 unstable transcripts (CUTs) and stable unannotated transcripts (SUTs), which in
255 normal conditions are expressed at a very low level (Wyers *et al.*, 2005; Marquardt,
256 Hazelbaker and Buratowski, 2011). Most CUTs are detectable only upon the
257 inactivation of the 3'-5' exonuclease Rrp6 subunit of the nuclear exosome (Xu *et al.*,
258 2009) and for this reason, only a handful of CUTs were detected in our RNA-seq
259 analysis of the *ceg1-AA* strain. Thus, we focused our investigation on the well-studied
260 ncRNA *CUT542* (*NEL025c*). The nuclear depletion of Ceg1 increased the levels of
261 *NEL025c* (Fig. 2H) up to 10 times after 120 min of rapamycin treatment, consistent
262 with the fact that lowly expressed Pol II transcripts accumulate when capping enzymes
263 are not functional. A similar effect was observed for *SUT238* (Fig. 2H).
264 Since the expression of non-caped mRNAs depends on their basal expression, we
265 tested whether the decrease in the RNA synthesis could alter the levels of *ADH1*
266 mRNA and *NEL025c* ncRNA observed upon Ceg1 nuclear depletion. To affect Pol II
267 elongation rate and processivity (Exinger and Lacroute 1992; Mason and Struhl 2005),
268 we treated cells with 6-azauracil (6-AU) for 30 min, which causes depletion of

269 intracellular nucleotide pools (Reines et al., 2003). This was followed by Ceg1 nuclear
270 depletion and analysis of the *ADH1* and *NEL025c* levels relative to the WT (Fig. 2I).
271 Slower RNA synthesis stabilised *ADH1* mRNA however, did not affect the
272 overexpression of *NEL025c* which suggests that the low expression of this gene
273 reached the threshold where further decrease had minimal impact on its accumulation.
274

275 **Degradation of non-capped Pol II transcripts**

276 Previous reports suggested that the decreased mRNA levels caused by capping
277 defects can be rescued by mutation of Rat1 exonuclease (Jimeno-González *et al.*,
278 2010). We employed *ceg1-63* and *ceg1-63/rat1-1* temperature-sensitive mutants to
279 assess the levels of highly expressed *ADH1* as well as *FMP27* genes previously used
280 to study capping-dependent RNA degradation (Jimeno-González *et al.*, 2010). *FMP27*
281 is a lowly expressed gene and therefore is placed under the *GAL1* promoter in the
282 *ceg1-63* background. We shifted the mutants and the parental strain to a non-
283 permissive temperature (37 °C) up to 120 min (for the analysis of *GAL1::FMP27* the
284 strain grew on galactose-containing medium). The mRNA levels of both *ADH1* and
285 *FMP27* decreased over time in *ceg1-63* however, the Rat1 inactivation in *ceg1-*
286 *63/rat1-1* did not rescue their abundance (Fig. 3A). The profile of the *FMP27* levels
287 expressed from the *GAL1* promoter were mirrored by the levels of endogenous *GAL1*
288 mRNA (Fig. 3A). In contrast to the temperature sensitive mutants *ceg1-63* and *ceg1-*
289 *63/rat1-1*, native *FMP27* mRNA expressed at low level did not decrease in *ceg1-AA*
290 but rather it remains stable (Fig. 3B). This may be caused by the difference in using ts
291 mutants versus rapid nuclear depletion to induce the capping defects as well as by a
292 significant difference between the expression from the native *FMP27* and *GAL1*
293 promoters. Moreover, expression from the latter was already affected in the WT cells

294 shifted to 37 °C. However, we cannot exclude that *FMP27* mRNA in *ceg1-63* is
295 rescued by Rat1 inactivation at the sub-permissive temperature (34 ºC) as previously
296 described (Jimeno-González *et al.*, 2010). The RNA levels of lowly transcribed ncRNA
297 *NEL025c* were not affected by the *rat1-1* mutation and increased in *ceg1-63/rat1-1*
298 (Fig. 3A).

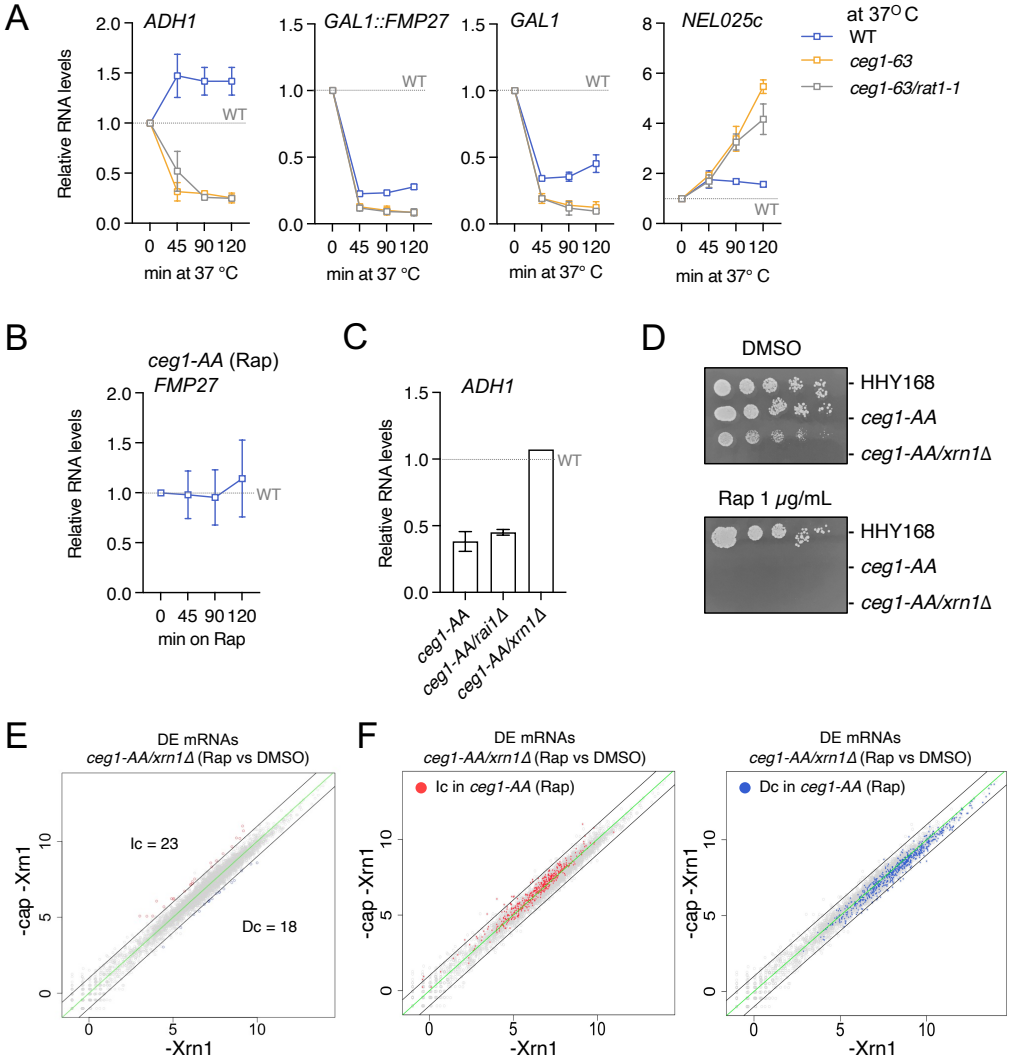

299

300 **Figure 3. Roles for 5'3' exonucleases in degradation of non-capped transcripts**

301 **A.** RNA levels of *ADH1*, *FMP27, GAL1* and *NEL025c* in WT and temperature-sensitive mutants *ceg1-*
302 *63* and *ceg1-63/rat1-1* after 0, 45, 90 and 120 min at a non-permissive temperature (37° C) compared
303 to control (WT at 25° C) set to 1 (dotted lines). For analysis of *GAL1:FMP27* and *GAL1* mRNAs cells
304 grew on gal-containing medium. **B.** *FMP27* mRNA levels in *ceg1-AA* after 0, 45, 90 and 120 min of
305 rapamycin treatment compared to WT (*ceg1-AA* on DMSO) set to 1 (dotted line). **C.** *ADH1* mRNA levels

306 in *ceg1-AA, ceg1-AA/rai1Δ* and *ceg1-AA/xrn1Δ* after 45 min on Rap compared to isogenic controls
307 growing on DMSO set to 1 (dotted line). **D.** Spot test showing the growth of *ceg1-AA/xrn1Δ* on DMSO
308 and rapamycin. Comparison with the growth of the parental strains *ceg1-AA* and HHY168. Serial
309 dilution of each strain was spotted on solid YPD media in the presence of DMSO or rapamycin at the
310 final concentration of 1 ug/mL. **E.** Differential expression of mRNAs after 45 min of rapamycin treatment
311 in *ceg1-AA/xrn1*Δ (-cap -Xrn1) compared to the control condition *ceg1-AA/xrn1*Δ on DMSO (-Xrn1).
312 Decreased (Dc) RNA species showing log2 fold change <1 are in blue. Increased (Ic) RNA species with
313 log2 fold change >1 are labelled in red. The zero-change line is in green. The black lines represent the
314 ±1 log2 fold change threshold. **F.** Increased (Ic) or decreased (Dc) mRNAs in *ceg1-AA* (Rap) are
315 labelled on the plot showing mRNA levels in *ceg1-AA/xrn1*Δ (Rap) compared to the control condition
316 *ceg1-AA/xrn1*Δ (DMSO)**. A-C.** RT-qPCR. The error bars show the standard deviation of three
317 independent experiments.
318
319 To avoid using the temperature-sensitive mutants we tested the Ceg1 nuclear
320 depletion combined with the deletion of the genes encoding the Rat1 binding partner
321 Rai1 (*ceg1-AA/rai1*Δ) or the exonuclease Xrn1 (*ceg1-AA/xrn1*Δ). The 5' to 3'
322 exonucleolytic degradation mediated by Rat1 and Xrn1 requires a monophosphate
323 RNA end (pRNA) while the RNA 5' ends generated by Pol II contain three phosphate
324 groups (pppRNAs) (Doamekpor et al., 2020; Jinek, Coyle, & Doudna, 2014).
325 Triphosphorylated 5' ends can be converted into proper substrates of the
326 exonucleases by Rai1 in the nucleus. Rai1 also stabilises and activates Rat1 by
327 forming a stable Rai1-Rat1 complex (Bresson and Tollervey 2018; Kachaev et al.
328 2020; Xiang et al. 2009). The Ceg1 nuclear depletion resulted in a similar decrease of
329 *ADH1* mRNA in strains with either functional or deleted *RAI1* (Fig. 3C). This further
330 confirmed that Rat1 is not efficiently involved in the degradation of non-capped
331 transcripts. In contrast, the deletion of *XRN1* rescued the levels of the non-capped
332 *ADH1* mRNA in *ceg1-AA* (Fig. 3C). Notably, the *ceg1-AA/xrn1Δ* strain grew slower

333 than WT and was non-viable on Rap-containing medium (Fig. 3D), underlining the
334 importance of m7G cap for cellular processes (e.g., translation).
335 The rescue effect observed for *ADH1* in *ceg1-AA/xrn1Δ* (Rap) prompted us to test
336 whether the differential expression in *ceg1-AA* could be rescued globally by the
337 deletion of the Xrn1 exonuclease. The *XRN1* null mutants were shown to stabilise non-
338 capped mRNAs in *CEG1* temperature-sensitive mutants (Schwer, Mao and Shuman,
339 1998). We performed global differential expression analysis on the *ceg1-AA/xrn1*Δ
340 strain growing on either DMSO (*xrn1Δ*) or Rap for 45 min. The Ceg1 nuclear depletion
341 in the *xrn1Δ* background resulted in only 18 decreased mRNAs, 13 of which were also
342 reduced in *ceg1-AA* (Rap) (Fig. 3E-F). Unexpectedly, the number of increased mRNAs
343 was also significantly lower compared to *ceg1-AA* as we detected only 23 upregulated
344 mRNAs (Fig 3E-F).
345 To elucidate why the *XRN1* deletion affected the accumulation of non-capped mRNAs
346 in Ceg1-depleted cells, we tested mRNA expression in *ceg1-AA/xrn1*Δ prior to the
347 nuclear depletion of Ceg1. We compared *ceg1-AA/xrn1*Δ (DMSO) to WT (*ceg1-AA* on
348 DMSO) and found that *XRN1* deletion results in a global change in the mRNA
349 expression, similar to the Ceg1 nuclear depletion. RNA-seq analysis revealed 543
350 upregulated and 605 downregulated mRNAs displaying log2 fold change < -1 and > 1
351 in *ceg1-AA/xrn1*Δ on DMSO (Fig. 4A). The upregulated genes were lowly expressed
352 (median log2 TPM = 2.6) while the decreased fraction was highly expressed (median
353 log2 TPM = 6.2) in WT cells (Fig. 4B). All of 1148 mRNAs differentially expressed in
354 *xrn1*Δ were split into three bins according to their expression levels in WT cells (Fig.
355 4C-D). The majority of the lowly expressed mRNAs increased (270 out of 282), while
356 most of the highly expressed mRNAs decreased (280 out of 282) in *xrn1Δ*. The
357 number of mid-range expressed genes was equally affected (268 upregulated, 296

358 downregulated) however, the median of their expression levels was overall decreased.
359 Consistently, upregulated genes displayed longer half-time compared to the
360 downregulated with a median of 30 min and 17 min, respectively (Fig. 4E). Next, we
361 tested if the effect of nuclear depletion of Ceg1 in *xrn1*Δ strain was masked by the pre-
362 existing aberrant accumulation of mRNAs caused by the only *XRN1* deletion. We
363 assessed how many differentially expressed mRNAs (log2 fold change < -1 and > 1)
364 in *ceg1*-AA were also differentially expressed in *xrn1*Δ prior to nuclear depletion of
365 Ceg1. We found that 190 out of 469 mRNAs increased and 264 out of 736 mRNAs
366 decreased in *ceg1-AA* were also increased or downregulated respectively in *xrn1*Δ
367 (Fig. 4F). This overlap identified only genes with log2 fold change over the ±1
368 threshold in both data sets therefore, we also tested the levels of differentially
369 expressed mRNAs in *ceg1-AA* in the total mRNA fraction in *xrn1*Δ. Generally, most of
370 the increased and decreased mRNAs identified in *ceg1-AA* were similarly affected in
371 *xrn1*Δ (Fig. 4G) displaying a mean log2 fold change of 1.28 for the increased and -
372 1.01 for the decreased mRNAs (Fig. 4H). We also performed reverse analysis and
373 tested the levels of increased and decreased mRNA in *xrn1*Δ (log2 fold change < -1
374 and > 1) on all mRNAs in *ceg1-AA* (Fig. 4I). Both groups are accordingly increased or
375 decreased in *ceg1-AA* (Rap) by a mean log2 fold change of 1.2 and -1.1 respectively
376 (Fig. 4J). This analysis indicates that both *XRN1* deletion and lack of capping
377 deregulate mRNA levels through a common mechanism and therefore the Xrn1 and
378 Ceg1 co-inactivation did not result in differentially expressed genes (Fig. 3E). Finally,
379 we compared the RNA-seq dataset from *ceg1-AA* (Rap) and *ceg1AA/xrn1*Δ (Rap) to
380 exclude the genes similarly affected by either *XRN1* deletion or Ceg1 depletion. We
381 identified 482 up- and 536 downregulated (Fig. S4A), both groups are similarly
382 expressed in WT cells (Fig. S4B).

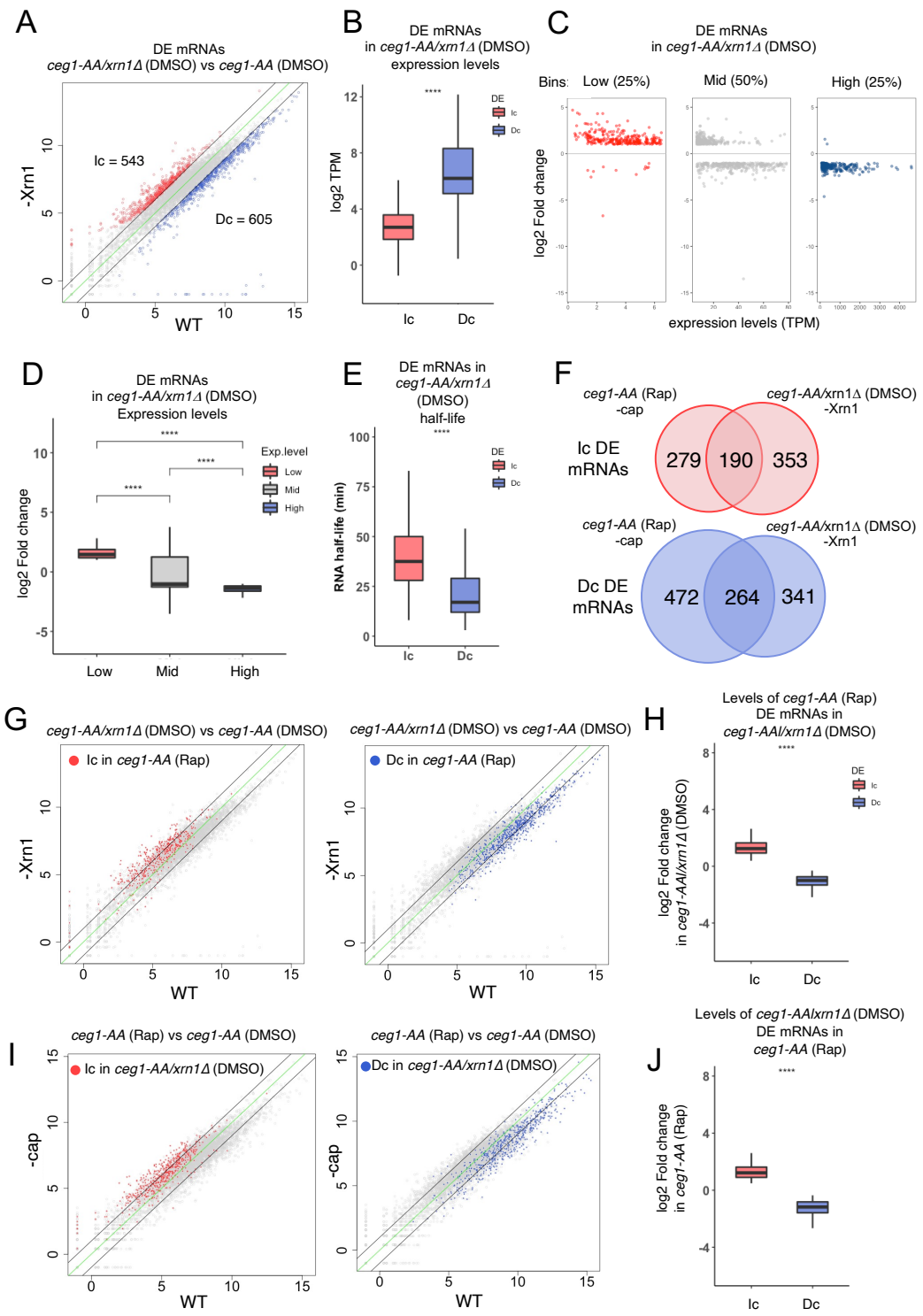

Figure 4. *XRN1* deletion and Ceg1 nuclear depletion similarly affect mRNA levels.

A. Differential levels of mRNAs in *xrn1Δ (ceg1-AA/xrn1Δ* on DMSO) compared to WT (*ceg1-AA* on DMSO). Increased (Ic) mRNAs with log2 fold change >1 are labelled in red, decreased (Dc) mRNAs showing log2 fold change <1 are in blue. The zero-change line is in green. The black lines represent the ±1 log2 fold change threshold. **B.** Differentially expressed mRNAs in *xrn1Δ* (*ceg1-AA/xrn1Δ* on

389 DMSO) sorted by their expression levels calculated by the log2 Transcript Per Million (log2 TPM) value
390 in WT (*ceg1-AA* on DMSO). **C.** The distribution of differentially expressed mRNAs in *xrn1*Δ depending
391 on their expression levels in WT cells. **D.** The overall fold change for differentially expressed mRNAs in
392 *xrn1*Δ ranked accordingly to their expression levels in WT cells. **E.** The half-life of differentially
393 expressed mRNAs in *xrn1*Δ (*ceg1-AA/xrn1*Δ on DMSO). **F.** The number of overlapping increased (Ic)
394 or decreased (Dc) mRNAs in *xrn1*Δ (*ceg1-AA/xrn1*Δ on DMSO) and *ceg1-AA* (Rap). **G.** Increased (red)
395 or decreased (blue) mRNA in *ceg1-AA* (Rap) are labelled on the plots showing mRNA levels in *ceg1-*
396 *AA/xrn1*Δ (DMSO) compared to the control condition (WT). **H.** The log2 fold change in *xrn1*Δ for the
397 sets of mRNAs that were differentially expressed in *ceg1-AA* (Rap). **I.** Increased (red) or decreased
398 (blue) mRNAs in in *xrn1*Δ are labelled on the plots showing mRNA levels in *ceg1-AA* (Rap) compared
399 to the control condition (WT). **H.** The log2 fold change in *ceg1-AA* (Rap) for the sets of mRNAs that
400 were differentially expressed in *xrn1*Δ.
401
402 Our data indicate that non-capped mRNAs are not subjected to any specific quality-
403 control degradation upon Ceg1 depletion, but they are rather degraded according to
404 their expression. This and the similarities with the *xrn1*Δ mutation suggest that the cap
405 structure is required for the processes of sensing and buffering the global mRNA levels
406 by Xrn1. Non-capped mRNAs are not rapidly degraded upon Ceg1 depletion as they
407 are not optimal substrates for the 5'-3' exonucleases and require modifications of the
408 5' ends by other enzymes. We hypothesise that such modifications are efficiently
409 performed if the capping enzymes are in place which may represent a condition for
410 the cap quality control to occur. In this scenario, even lowly expressed non-capped
411 mRNAs with a suitable 5' end would be efficiently removed in WT cells. To test this
412 hypothesis, we introduced the self-cleaving hepatitis delta virus (HDV) ribozyme
413 sequence into the 5' UTR of the *FMP27* gene (*fmp27-RZ)* (Fig. 5A). The internal self-
414 cleavage of *fmp27-RZ* generated a non-capped transcript with a 5'-OH end which is
415 a suboptimal substrate for 5'-3' exonucleases (Doamekpor et al., 2020; Jinek, Coyle,

416 & Doudna, 2014). As a control we used the catalytically inactive ribozyme mutant
417 harbouring the substitution C76:U (*fmp27-C76U*) (Perrotta, Shih and Been, 1999; Bird
418 *et al.*, 2005). *FMP27* levels did not change upon Ceg1 nuclear depletion (Fig. 3B).
419 However, in WT cells the introduction of the HDV ribozyme decreased the levels *of*
420 *fmp27-RZ* by 64% compared to the catalytically inactive *fmp27-C76U* (Fig. 5B). This
421 indicates that the generation of the correct substrate for exonucleases was required
422 for the quality control and efficient degradation as previously reported (Bresson and
423 Tollervey 2018).

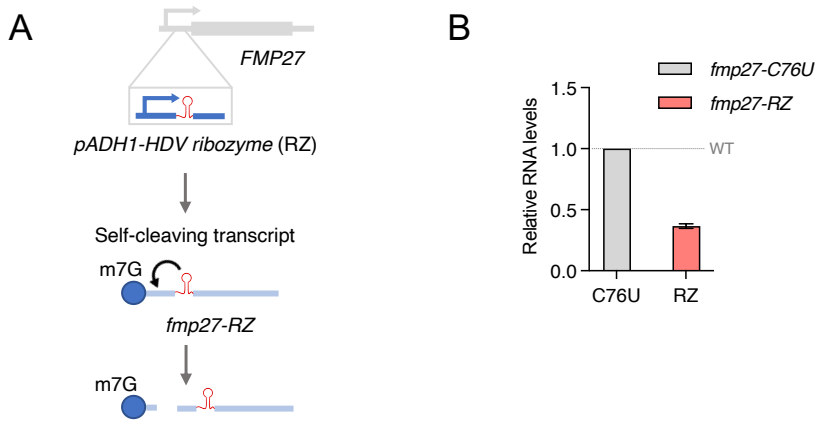

424

425 **Figure 5. Cap removal is required for 5'-3' degradation.**

426 **A.** The experimental approach for the generation of the self-cleaving *fmp27-RZ* transcript. **B.** The
427 mRNA levels of *fmp27-RZ* and *fmp27-C76U* mutants. The error bars show the standard deviation of
428 three independent RT-qPCR experiments.

429

430 **Non-capped mRNAs are not prematurely terminated**

431 Although efficient co-transcriptional degradation is required for termination, previous
432 studies reported that shifting the temperature-sensitive mutant *ceg1-63* to sub-
433 permissive temperature resulted in a premature transcription termination of the 8 kb-
434 long gene *FMP27* (Jimeno-González *et al.*, 2010). This effect was not fully
435 recapitulated in the *ceg1-AA* strain. Our ChIP analysis using an antibody recognizing

436 Pol II CTD revealed only a slight reduction of Pol II occupancy 0.5 kb from the
437 transcription start site but not further downstream of the gene (Fig. 6A). Since the
438 average gene length in yeast is 1.4 kb (Hurowitz and Brown, 2003), we investigated
439 how transcription was affected by Ceg1 nuclear depletion on shorter genes (Fig 6B).
440 We depleted Ceg1 for 45 min and analysed the distribution of Pol II phosphoisoforms
441 on highly and lowly expressed genes: *ADH1* and *PML39*, respectively (Fig. 6C-D).
442 ChIP analysis revealed that total Pol II was partially depleted mainly on the 5' ends for
443 both highly and lowly expressed genes. We used 8WG16 antibody recognising non-
444 modified heptapeptides of the CTD to analyse total Pol II distribution. Thus, we
445 speculate that this decrease of the Pol II signal detected by this antibody may reflect
446 prematurely terminated unphosphorylated or hypophosphorylated Pol II. Indeed, both
447 ser5-P and ser2-P Pol II phosphoisoforms, that represent actively transcribing Pol II,
448 were only marginally affected by Ceg1 depletion (Fig. 6C-D).
449 A similar but less pronounced effect was observed for *ADH1* gene in *cet1-AA* (Rap)
450 (Fig. S4A) as both enzymes are essential for cap formation (Martinez-Rucobo *et al.*,
451 2015). Nuclear depletion of Abd1 did not affect the distribution of Pol II over *ADH1*
452 (Fig. S4B). We also investigated if longer nuclear depletion of Ceg1 resulted in
453 increased premature transcription termination. We shifted cells to the medium
454 containing Rap for up to 120 min and tested the levels of Pol II over the 3' end of high
455 and mid-range expressed *ADH1*, *PYK1* and *PMA1* genes (Fig. 6E). Consequently, we
456 observed only ~20% decrease in Pol II signal at 45 min which was not exacerbated
457 by longer nuclear depletion of Ceg1.
458

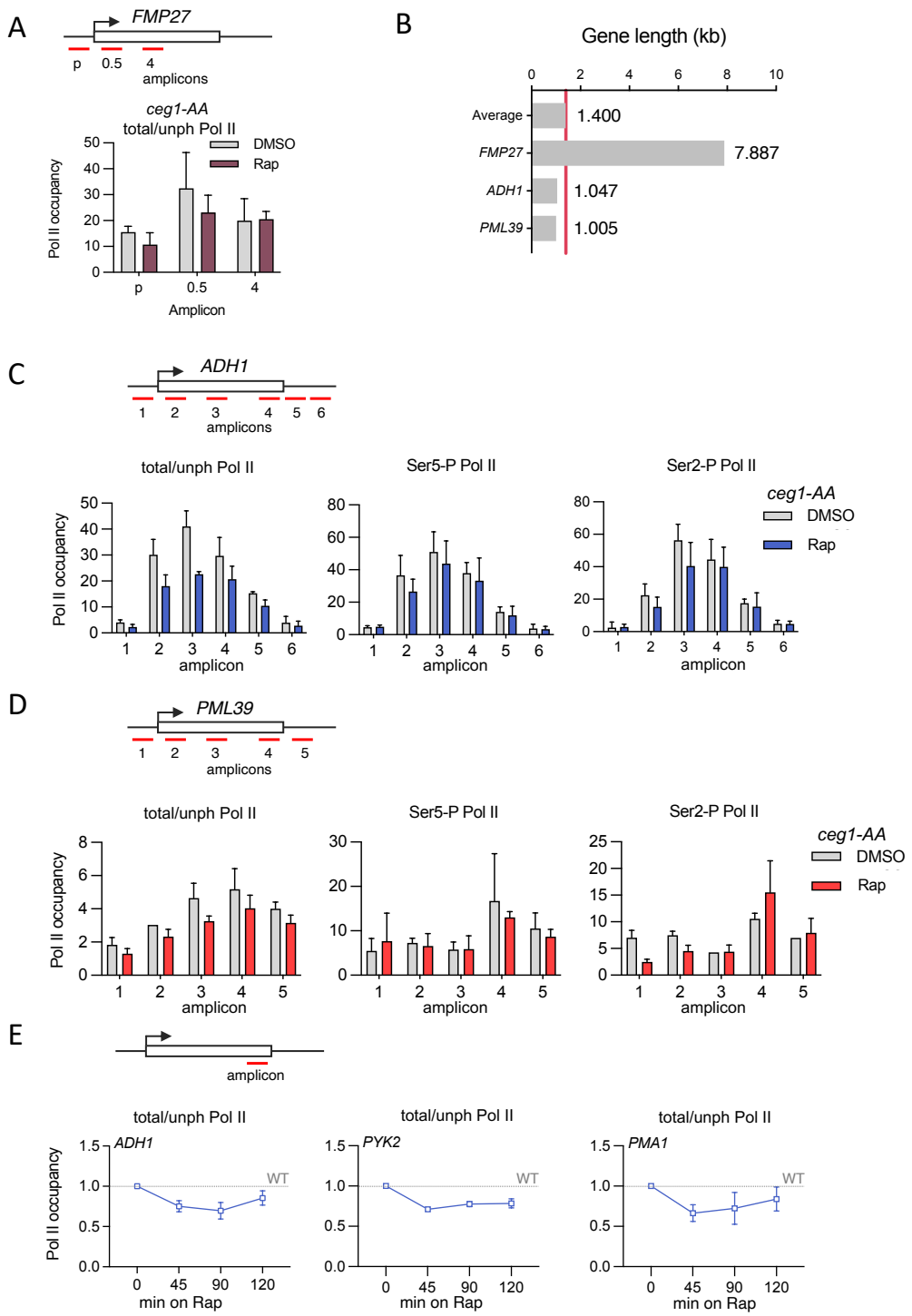

Figure 6. Transcription of non-capped mRNAs is not disrupted by pre-mature termination. **A.** The distribution of total/unphosphorylated Pol II (total/unph Pol II) over *FMP27* in control (DMSO) and after 45 min of rapamycin treatment (Rap) in *ceg1-AA*. The location of the amplicons used for the ChIP-qPCR over *FMP27* is shown above the chart. The error bars show the standard deviation of three independent ChIP-qPCR experiments. **B.** Chart showing the length of FMP27, *ADH1* and *PML39* genes. The red line represents the average gene length in *S. cerevisiae* (1.4 kb). **C-D.** The distribution

466 of total/unphosphorylated Pol II (total/unph Pol II) as well as serine 5-phosphorylated (Ser5-P Pol II)
467 and serine 2-phosphorylated (Ser2-P Pol II) Pol II isoforms over *ADH1 (C)* and *PML39* (D) in control
468 (DMSO) and after 45 min of rapamycin (Rap) in *ceg1-AA* strain. The location of the amplicons used for
469 the ChIP-qPCR is shown above the charts. The error bars show the standard deviation of three
470 independent ChIP-qPCR experiments. **E.** The occupancy of the total/unphosphorylated Pol II at the 3'
471 end of *ADH1, PYK2* and *PMA.* Timepoints after 0, 45, 90 and 120 min on rapamycin compared to
472 control (*ceg1-AA* on DMSO) and set to 1 (dotted line). The location of the amplicons used for the ChIP-
473 qPCR is shown above the charts. The error bars show the standard deviation of three independent
474 ChIP-qPCR experiments.
475

476 **DISCUSSION**

477 Capping is the first co-transcriptional RNA modification posed on the mRNAs. The
478 m7G cap is essential for the functionality of the mRNA and therefore, mutations
479 affecting the cap formation are non-viable. Previous studies reported that RNAs with
480 defective caps (e.g. lacking m7G or with non-methylated caps) are rapidly degraded
481 by cap quality control mechanisms, however, these analyses were performed only on
482 a few selected genes (Lewis and Izaurralde, 1997; Schwer, Mao and Shuman, 1998;
483 Cougot *et al.*, 2004; Topisirovic *et al.*, 2011). Here, we performed a global analysis of
484 the capping defective transcriptome. We show that although the overall mRNA levels
485 decrease was a dominant effect following the nuclear depletion of the capping
486 enzymes, the levels of many mRNAs did not change and strikingly, some of the
487 mRNAs increased when not capped. Our data show a clear dependence between the
488 amount of RNA synthesised, stability and the degradation of uncapped transcripts.
489 The nuclear depletion of Ceg1 resulted in the depletion of highly expressed mRNAs
490 and accumulation of lowly expressed and more stable mRNAs. We observed the same
491 pattern in cells lacking the 5'-3' exonuclease Xrn1 which is the major enzyme
492 degrading mRNA in the cytoplasm. Consistently, we did not detect any significant

493 number of differentially expressed genes in the *xrn1Δ* strain following nuclear
494 depletion of Ceg1. These observations allowed us to draw a few conclusions. First,
495 our data indicate that non-capped mRNA is not quality controlled but randomly
496 degraded. Therefore, the most abundant and so most accessible RNA species
497 decrease upon nuclear depletion of the capping machinery. This in turn, may increase
498 the relative concentration of lowly transcribed mRNAs in the overall fraction which we
499 detected as upregulated mRNAs. We speculate that the m7G cap may not be essential
500 for the protection from exonucleolytic 5'-3' degradation upon Ceg1 depletion, as the 5'
501 triphosphate non-capped mRNAs synthesised are not immediate substrates of the 5'-
502 3' exonucleases. Cells have mechanisms that convert different variants of RNA 5'
503 ends to substrates for exonucleases. For example, Rai1 shows both decapping
504 and pyrophosphohydrolase activity which generates monophosphate RNA 5' end
505 (pRNA) substrate of its binding partner, the 5'-3' ribonucleases Rat1 (Xiang *et al.*,
506 2009; Jiao *et al.*, 2010). However, the depletion or inactivation of these proteins did
507 not rescue the mRNA levels in Ceg1-depleted cells, indicating that the Rai1-Rat1
508 complex is not efficiently involved in their degradation. Similarly, the levels of nuclear
509 CUT and SUT tested in this study increased upon simultaneous Ceg1 depletion and
510 Rat1 inactivation. The lack of a specific degradation pathway targeting the RNAs
511 synthesised without the cap may aid the production of other essential RNA classes
512 produced by the RNA Pol I and III such as ribosomal RNA (rRNA) or transfer RNA
513 (tRNA), respectively, that are not capped but stable in the nucleus and cytoplasm
514 (Ramanathan, Robb and Chan, 2016; Akiyama, Eiler and Kieft, 2017). In these cases,
515 the synthesis would not be affected by the surveillance mechanisms degrading non-
516 capped RNAs in the nucleus. However, releasing and maintaining non-functional
517 mRNAs may have deleterious effects on the cell. Thus, we speculate that the binding

518 of the capping enzymes to the transcriptional machinery or the synthesis of the m7G
519 cap itself, is the condition required for the cap quality control pathway to be functional.
520 Indeed, the insertion of the self-cleaving ribozyme into the 5' UTR of *FMP27* resulted
521 in degradation of this lowly transcribed mRNA in WT cells.
522 Cap may be essential for the Xrn1-dependent buffering of the global mRNA levels.
523 Decapping enzymes interact with Xrn1, and the cap removal is the first step triggering
524 mRNA degradation (Schoenberg and Maquat, 2012). Thus, non-capped mRNAs may
525 not be identified as coding transcripts and therefore subjected to level correction. The
526 hypothesis that the cap is required for efficient mRNA degradation and buffering of the
527 mRNA levels is supported by the observation of a similar pattern in the mRNA levels
528 in the strain lacking Xrn1. Almost all genes upregulated and downregulated upon Ceg1
529 nuclear depletion were also respectively affected in the *xrn1*Δ strain. We speculate
530 that the lack of the cap may disturb the correct buffering of mRNA levels (Fig. 7) and
531 thus mRNAs are degraded randomly by cytoplasmic degradation enzymes like the
532 exosome.

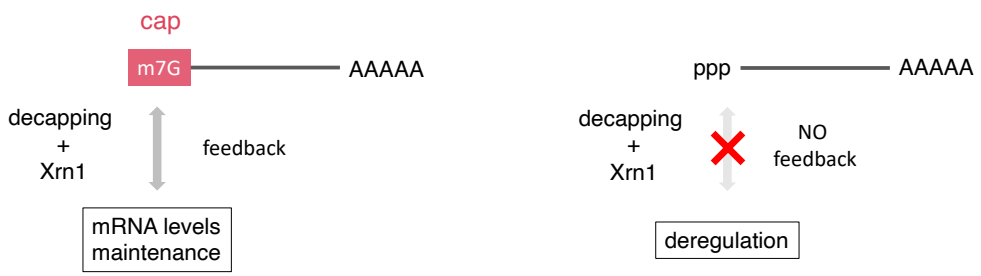

533

534 **Figure 7. A model of cap-dependent regulation of mRNA levels**

535

536 Indeed, the cap plays a role in marking the Pol II-dependent transcripts. For example,
537 the presence of the cap at the 5' end decides the fate of yeast box C/D snoRNAs, a
538 class of RNAs which do not possess the m7G cap as mature species. However, when
539 their 5' end processing is affected and the cap retained, these snoRNAs are subjected

540 to mRNA processing pathways, become polyadenylated at the 3' end as well as
541 exported to the cytoplasm (Grzechnik *et al.*, 2018). Similarly, the cap structure may
542 mark the mRNAs as coding transcripts facilitating the homeostatic adjustments in their
543 levels by degradation and synthesis.
544 Finally, we did not observe a significant increase in premature transcription termination
545 upon depletion of the capping enzymes. This is consistent with our data showing that
546 Rat1 and Rai inactivation did not restore the levels of non-capped mRNAs, but in
547 contrasts with previous models suggesting that such RNAs are degraded co-
548 transcriptionally by Rat1 eliciting the removal of Pol II from DNA by the "torpedo
549 termination" mechanism, where 5'-3' exonuclease Rat1 attacks the 5' unprotected
550 end, chases the Pol II by degrading the nascent RNA, and ultimately displaces the
551 transcribing polymerase from the DNA template (Eaton et al., 2020; Kim et al., 2004;
552 West, Gromak, and Proudfoot, 2004). Our ChIP analysis revealed that only the fraction
553 of Pol II tested using 8WG16 antibody was slightly depleted in *ceg1-AA* (Rap). This
554 antibody recognises unphosphorylated heptapeptides in the CTD and therefore the
555 precipitated fraction may be enriched for hypophosphorylated Pol II. Such Pol II may
556 not efficiently transit to the elongation phase, pause or transcribe at a low speed
557 (Bartkowiak and Greenleaf, 2011; Harlen *et al.*, 2016; Harlen and Churchman, 2017).
558 All these conditions facilitate transcription termination by a torpedo mechanism, which
559 may contribute to the lowered levels of Pol II observed in the ChIP analyses employing
560 8WG16 antibody. We speculate that for average length genes (1.4 kb) the window in
561 which Rai-Rat1 can be recruited to the transcribing complex and thus catch normally
562 transcribing Pol II is too narrow to trigger transcription termination upstream of the
563 canonical transcription end site. Alternatively, the capping process must be at least
564 initiated, and the capping enzymes present on the transcribing complex to facilitate

565 the quality control mechanism. For example, premature transcription termination is
566 observed when nascent RNAs are decapped which triggers Pol II pausing and
567 consequent Rat1-dependent termination (Brannan *et al.*, 2012; Contreras, Benkirane
568 and Kiernan, 2013; Eaton and West, 2020; Eaton *et al.*, 2020). Such condition would
569 be consistent with our hypothesis that the major role of the cap is marking the mRNA
570 as a product of the Pol II and coding RNAs in the cytoplasm.
571 Overall, our work indicates that the 5' cap role is more complex than serving as a
572 platform for the Cap Binding Complex and punctuating mature 5' ends of Pol II
573 transcripts. Cap may play an essential role in marking mRNA molecules and
574 cooperating with Xrn1-dependent buffering of the cellular mRNA levels.
575

576 **ACKNOWLEDGMENTS**

577 This work was funded by Sir Henry Dale Fellowship from the Wellcome Trust and the
578 Royal Society (218537/Z/19/Z). O.Z. was supported by Midlands Doctoral Training
579 Partnership by a studentship to O.Z. funded by BBSRC (grant number:
580 BB/M01116X/1). DH is funded by EPSRC (grant EP/T002794/1). We thank Kinga
581 Winczura, Lauren Garbett and Mark Ashe for critical reading of the manuscript and
582 Genomics Birmingham at the University of Birmingham for assistance with NGS.
583

584 **CONFLICT OF INTEREST**

585 The authors declare that they have no conflict of interest.
586

587 **AUTHOR CONTRIBUTION**

588 O.Z. performed all experiments, bioinformatics and analysed data. D.H. supported
589 bioinformatics. P.G. and O.Z. designed experimental approaches and wrote the
590 manuscript.
591
592 **MATERIALS AND METHODS**
593 **Data availability**
594 The RNA-seq data for the *ceg1-AA* strain upon 45 min of treatment with DMSO or
595 rapamycin are available in Gene Expression Omnibus (GEO) database with the
596 accession number GSE213942 .
597
598 **Yeast strain and Media**

Strain	Genotype	Source
HHY168	MATalpha tor1-1 fpr1::NAT RPL13AxFKB12::TRP	Euroscarf
ceg1-AA	MATalpha tor1-1 fpr1::NAT RPL13AxFKB12::TRP CEG1-FRB::HIS	This work
cet1-AA	MATalpha tor1-1 fpr1::NAT RPL13AxFKB12::TRP CET1-FRB::HIS	This work
abd1-AA	MATalpha tor1-1 fpr1::NAT RPL13AxFKB12::TRP ABD1-FRB::HIS	This work
cbp20-AA	MATalpha tor1-1 fpr1::NAT RPL13AxFKB12::TRP CBP20-FRB::HIS	This work

cbp80-AA	MATalpha tor1-1 fpr1::NAT RPL13AxFKB12::TRP CBP80-FRB::HIS	This work
ceg1-AA/xrn1Δ	MATalpha tor1-1 fpr1::NAT RPL13AxFKB12::TRP CEG1-FRB::HIS KAN::XRN1	This work
ceg1-AA/rrp6Δ	MATalpha tor1-1 fpr1::NAT RPL13AxFKB12::TRP CEG1-FRB::HIS KAN::RRP6	This work
ceg1-63	MATa ceg1Δ::HIS3 PGAL1-YLR454::URA3 ura3Δ [pRS315-ceg1-63]	(Jimeno-González *et al.*, 2010)
ceg1-63/rat1-1	MATa rat1-1 ceg1Δ::HIS3 PGAL1-YLR454::URA3 ura3Δ [pRS315-ceg1-63]	(Jimeno-González *et al.*, 2010)
fmp27-C76U	MATalpha tor1-1 fpr1::NAT RPL13AxFKB12::TRP CEG1-FRB::HIS URA3::RZc76u::YLR454	This work
fmp27-RZ	MATalpha tor1-1 fpr1::NAT RPL13AxFKB12::TRP CEG1-FRB::HIS URA3::RZ::YLR454	This work
ceg1-AA/rai1Δ	MATalpha tor1-1 fpr1::NAT RPL13AxFKB12::TRP CEG1-FRB::HIS KAN::RAI1	Thhis work

599

600 Yeast strains were grown at 30° C on YPD (1% yeast extract, 2% peptone, 2%
601 dextrose/glucose) media enriched in DMSO or rapamycin to the final concentration of
602 1 µg/mL where indicated. For 6-AU treatment, the yeast cells were grown in minimal
603 media (yeast nitrogen base without amino acids) with synthetic dropout ura-. For solid
604 media, agar was added to the final concentration of 2%.
605
606 **Growth spot assay**
607 Yeast cells were grown to OD600 = 0.4. Serial dilutions 1 :25 were performed and 5
608 µL of each dilution spotted onto YPD (2% agar) plates.
609
610 **Yeast cell transformation**
611 Cells were cultured to OD600 = 1 and pelleted by centrifugation for 5 min at 2 400 x g
612 at room temperature (RT). The pellet was resuspended in sterile 10 mM Tris-HCl pH
613 7.5 or water and centrifuged again as before. The pellet was resuspended in filtered
614 LiT (10 mM Tris-HCl pH 7.5;100 mM Lithium acetate), 1 M DTT and incubated at RT
615 for 40 min with gentle shaking. After incubation the cells were pelleted again (as
616 before) and resuspended in LiT and 1 M DTT. The suspension was added with LiT;
617 and dsDNA (10 mg/mL); transforming DNA (0.1 to 1 ug or more) and incubated at RT
618 for 10 min. Next, PEG solution (1:1 PEG4000 : LiT) was added to the suspension and
619 incubated at RT for 10 min. DMSO was then added, and the suspension incubated at
620 42° C for 15 min. After the incubation the suspension was pelleted and resuspended
621 in 1 mL of YPD (1% Bacto yeast extract, 2% Bacto peptone, 2% glucose/dextrose).
622 Then the suspension was incubated at 30° C for 1 hour, pelleted with 10 seconds (sec)
623 spin, max speed and inoculated on selective plates.
624

625 **RNA extraction**

626 RNA was purified by phenol/chloroform method. The yeasts were cultured to the final
627 concentration OD600 = 1, pelleted in 50 mL falcon tubes by centrifugation for 2 min at
628 1000 rpm at room temperature (RT). The pellet was frozen at -80° C before further
629 manipulation. Next, the pellet was resuspended in 1 mL of ice-cold RNase free water,
630 moved to a 1.5 mL tube, centrifuged for 10 sec at 4° C max speed. Then the
631 supernatant (water) was removed, and the pellet resuspended in 400 µL of filtered AE
632 buffer (50mM Sodium acetate pH5.3; 10mM EDTA), 40 µL of 10% Sodium dodecyl
633 sulphate (SDS) and 400 µL of Acid Phenol (pH 4). The suspension was vortexed for
634 20 sec and incubated at 65° C for 10 min, then incubated for further 10 min at -80° C.
635 The defrosted sample was then centrifuged for 5 min, 13 000 rpm at RT. 400 µL of 1:1
636 phenol:chloroform solution were added to the supernatant and vortexed for 30 sec.
637 Then the sample was centrifuged 10 min, 13 000 rpm at RT. The upper phase was
638 transferred and mixed with 400 µL of Chloroform, vortexed and centrifuged for 5 min,
639 13 000 rpm at RT. The RNA was precipitated by adding to the upper phase 1 mL of
640 100% ethanol and 40 µL of 7.5 M Ammonium acetate. Left at -80° C for 2 hours (hrs)
641 then centrifuged for 20 min, 13 000 at 4° C. The pellet was washed with 70% ethanol
642 (in water) and resuspended in RNase free water.

643

644 **RT-qPCR**

645 Reverse transcription was performed with Super Script III Reverse transcriptase
646 (Thermo Fisher, 18080044) following manufacturer's instruction using random
647 hexamers (Thermo Fisher, N8080127) for cDNA synthesis. qPCR data were analysed
648 with the ΔΔCt method normalised to 25S ribosomal RNA (rRNA) and control condition.

649

650 **RNA sequencing**

651 Before library preparation, ribosomal RNA (rRNA) depletion was performed on 5 µg of
652 total yeast RNA using 200 pmol of 3' biotinylated probes (IDT) designed in house
653 following the RiboPOP method (Thompson, Kiourlappou, and Davis 2020). The
654 libraries preparation was performed with Ultra II RNA Library Prep Kit for Illumina
655 (NEB, E7770) and Multiplex Oligos for Illumina (NEB, E7335) according to
656 manufacturer's instructions. The RNA sequencing was performed from the Genomics
657 Facility at the University of Birmingham on Illumina NEXTseq apparatus.

658

659 **RNA-seq data analysis**

660 The quality of the data was checked using FastQC v0.11.5 (Andrews S. (2010).
661 FastQC: a quality control tool for high throughput sequence data. Available online at:
662 http://www.bioinformatics.babraham.ac.uk/projects/fastqc).
663 Reads were aligned to the yeast genome R64 (sacCer3) using HISAT2 v2.1.1 and
664 sorted and indexed using SAMtools v1.15.1 (Wysoker et al. 2009). The read count per
665 gene were calculated with LiBiNorm v.2.5 (Dyer, Shahrezaei and Hebenstreit, 2019)
666 with the following parameters count -u name-root -f --order=pos --minaqual=10 --
667 mode=intersection-strict --idattr=gene_id --type=exon. Differential expression analysis
668 was performed using DESeq2 package. GO analysis was generated using g:profiler
669 (https://biit.cs.ut.ee/gprofiler).

670

671 **Cap Immunoprecipitation**

672 Total RNA from cells treated with DMSO or rapamycin was extracted and use for cap
673 pull-down. 5 µg of total yeast RNA was spiked with 1 µg of total human RNA as
674 immunoprecipitation efficiency control. Capped RNA species were

675 immunoprecipitated using 5 µg of anti m7G cap antibody (H-20) as previously
676 described (Jimeno-González et al. 2010).
677
678 **6-azauracil (6-AU) treatment**
679 Overnight culture was prepared inoculating a single colony on minimal media as
680 described above. The next day the culture was diluted to OD600 = 0.2. The diluted
681 culture was grown with agitation at 30° C to OD600 = 1 and split in 4. Two cultures
682 were added of 6-azauracil (6-AU) and the other two with ammonium hydroxide
683 (NH4OH, control) at the final concentration of 50 µg/mL for 30 min. Next, DMSO or
684 rapamycin (Rap) at the final concentration of 1 µg/mL were added according to the
685 following scheme: 6-AU+DMSO, 6-AU+Rap, NH4OH+DMSO, NH4OH+Rap. 10 mL of
686 each suspension were collected a time 0, 45, 90 and 120 min after the addition of
687 DMSO or Rap and prepared for RNA purification.
688
689 **4-Thiouracil (4tU) labelling and purification**
690 Liquid yeast culture traded for 40 min with rapamycin (1 µg/mL) or DMSO were added
691 of 4tU 500 µM final concentration (Sigma-Aldrich, 440736) to final concentration 5 mM
692 for 5 min and subsequently flash frozen in cold ethanol (-80° C). The suspension was
693 pelleted RNA purified by Phenol/Chloroform extraction. 200 µg of total RNA from *S.*
694 *cerevisiae* was spiked with *S. pombe* total RNA (4:1 ratio *S. cereviasiae* : *S. pombe*)
695 treated with 4-tU 500 µM final concentration (Sigma-Aldrich, 440736). The biotinylation
696 was performed with 200ul EZ-link-HPDP-biotin (Thermo Fisher, 21341) for 30 min at
697 65° C. The RNA was then incubated with 5M sodium chloride and isopropanol and
698 incubated with Dynabeads M-270 Streptavidin (Thermo Fisher, 65305) for 1 hour at
699 room temperature. Beads were washed five times with Binding & Washing buffer (5

700 mM Tris-HCl pH 7.5, 0.5 mM EDTA and 1 M NaCl) and 4tU labelled-RNA was eluted
701 with 100 μM DTT, precipitated with 5M NaCl, isopropanol and glycogen, and
702 resuspended DNase/RNase free water. Enrichment of nascent RNA was confirmed
703 with qPCR using exon–intron primers of ACT1 gene.
704
705 **Chromatin immunoprecipitation (ChIP)**
706 The specific yeast strain was grown over-night to OD600 = 1. Then 37% formaldehyde
707 was added to the media to final concentration 1% dropwise with gentle shaking for 15
708 min. Next, 15 mL of 2.5 M glycine was added for further 5 min keeping the shaking.
709 The cells were pelleted by centrifugation at 3 500 rpm for 3 min at 4° C. The pellet was
710 resuspended in 40 mL of ice-cold 1x PBS and centrifuged at 3 500 rpm for 5 min at 4°
711 C, twice. The pellet obtained was then transferred and prepared for lysis. The pellet
712 was resuspended in 1 mL of ice-cold FA1 (50 mM HEPES-KOH, pH7.5; 150 mM NaCl;
713 1 mM EDTA; 1% triton-x 100; 0.1% Sodium deoxycholate) added with proteinase
714 inhibitor (Roche Mini-EDTA free) and about 400 μL zirconia beads. The cells were
715 lysed in MagnaLyser (30 sec 7000 rpm, 3 cycles with 5 min incubation on ice in
716 between). The lysate was drained out of the beads by centrifugation 1 000 rpm for 1
717 min at 4° C and SDS was added to a final concentration of 0.05%. The lysate was
718 sonicated as follow: 25 cycles 15 sec ON, 15 sec OFF on maximum power. Next, it
719 was centrifuged for 20 min at 12 500 rpm at 4° C. 200 μL of lysate was saved to check
720 the fragmentation. SDS was added to the lysate with to final concentration of 1% and
721 0.05 mg of Proteinase K and incubated at 42° C for 1 hour. Next it was moved to 65°
722 C for 4 hrs. The DNA de-crosslinked was precipitated by Phenol/Chloroform, the
723 contaminant RNA removed by adding 2 μL of RNase A incubating for 1 hour at 37° C
724 and checked on agarose gel. The rest of the lysate was centrifuged max speed for 5

725 min at 4° C. 150 µg of chromatin were used for immunoprecipitation. FA1 enriched
726 with proteinase inhibitor was added to the DNA to a final volume of 700 µL. 20 µL of
727 such mix was saved as input for the further ChIP analysis. 2 µg of the specific antibody
728 was added to the sample and incubated on rotation over-night at 4° C.
729 15 µL of protein A (Thermo Fisher, 10002D) and 15 µL of protein G-coated beads
730 (Thermo Fisher, 10004D) were washed with 1 mL of FA1 and resuspended in 100 µL
731 of FA1. The beads were added to the sample and incubated by rotation for 1 hour at
732 4° C. After incubation the beads were washed 6 times with FA1, 1 time with FA2 (50
733 mM HEPES-KOH, pH 7.5; 500 mM NaCl; 1 mM EDTA; 1% Triton-X 100; 0.1% Sodium
734 deoxycholate), 1 time with FA3 (20 mM Tris pH 8.0; 250 mM LiCl; 0.5% NP-40; 0.5%
735 Sodium deoxycholate; 1 mM EDTA) and TE buffer pH 8 (100 mM Tris-HCl; 10 mM
736 EDTA). The beads were then resuspended in 195 µL of Elution buffer (50 mM Tris pH
737 7.5; 10 mM EDTA; 1% SDS) and incubated for 10 min at 65° C and 0.05 mg of
738 Proteinase K added. The Chromatin was then de-crosslinked by incubating the sample
739 at 42 ° C for 1 hour and moved at 65° C for 4 hrs. The DNA was finally purified using
740 Quiagen cleanup (28104) kit following the manufacturer's instruction.
741
742
743
744
745
746
747
748
749

750 **SUPPLEMENTAL FIGURES**

751

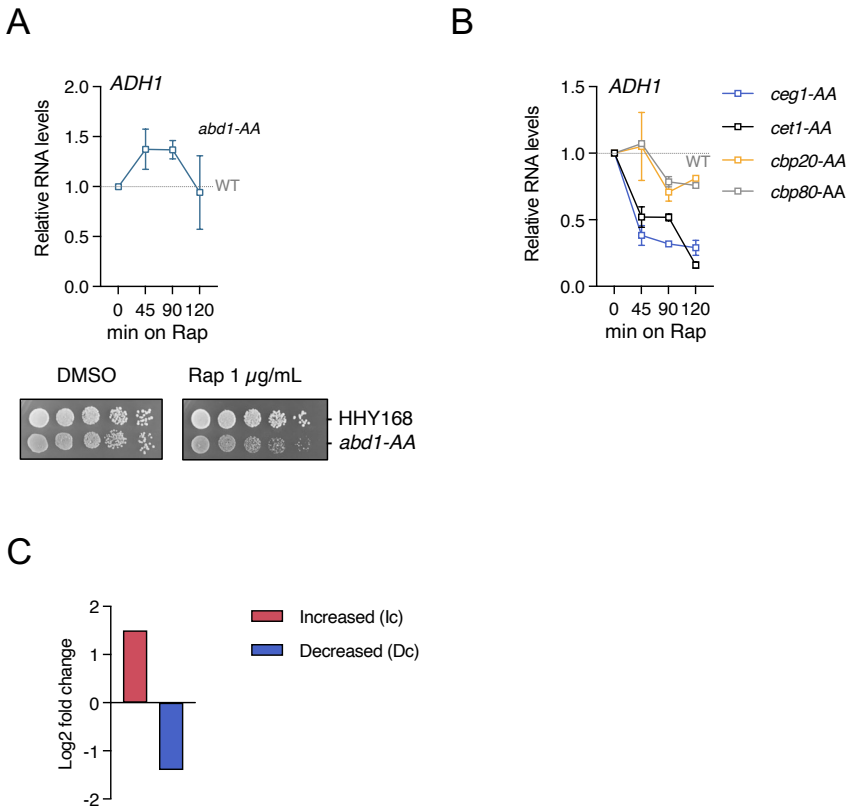

752

753 **Figure S1.**

754 **A.** *ADH1* mRNA levels time during nuclear depletion of Abd1. RT-qPCR RNA levels at 0, 45, 90 and
755 120 min of rapamycin treatment relative to control (top). The error bars show the standard deviation of
756 three independent experiments. Spot test showing the growth of *abd1-AA* strain on DMSO and Rap
757 (bottom) in comparison with to the parental strain HHY168. Serial dilution of each strain was spotted on
758 YPD media in the presence of DMSO or rapamycin at the final concentration of 1 ug/mL. **B.** *ADH1*
759 mRNA levels during nuclear depletion of Ceg1, Cet1, Cbp20 and Cbp80. RT-qPCR showing the RNA
760 levels measured at 0, 45, 90 and 120 min of rapamycin treatment relative to control (DMSO). The error
761 bars show the standard deviation of three independent experiments. **C.** Bar chart showing the average
762 fold change for decreased (D) and increased (I) mRNA species upon Ceg1 nuclear depletion.

763

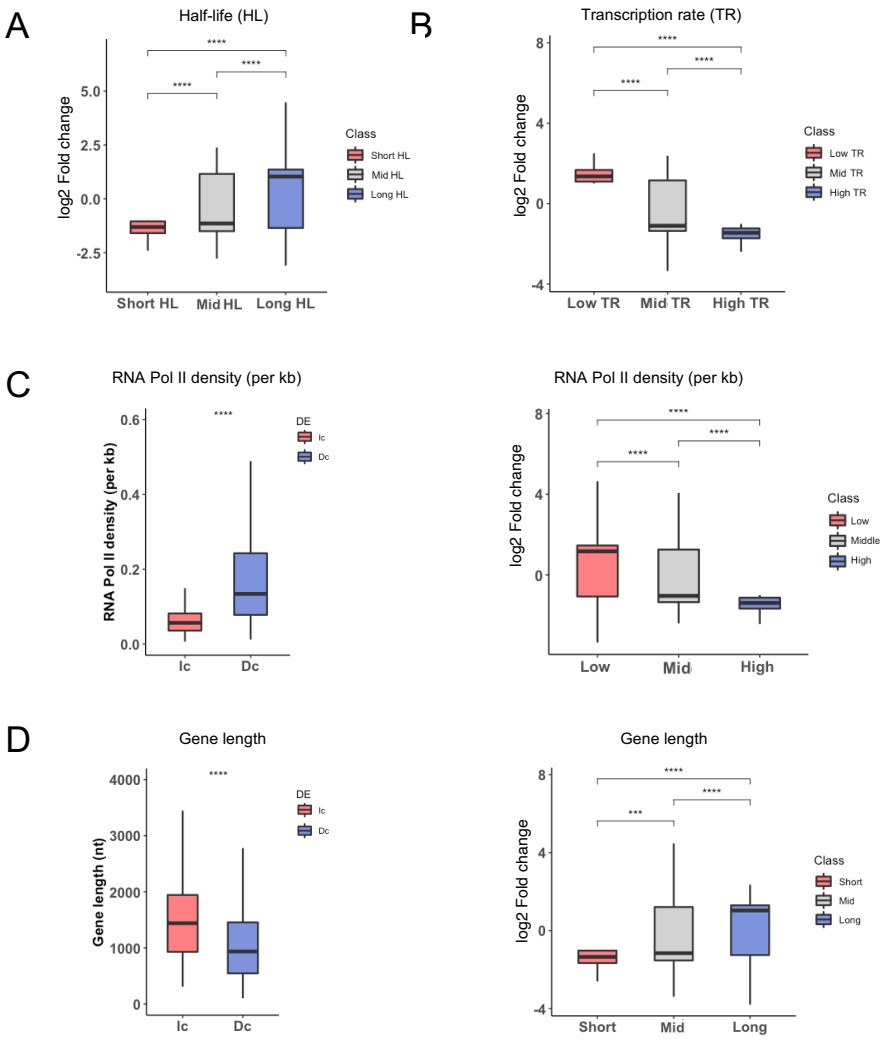

Figure S2.

A-D. Fold change and fold change sorted by the expression level in *ceg1-AA* (DMSO) for differentially accumulated mRNAs in *ceg1-AA* (Rap) vs *ceg1-AA* (DMSO) plotted accordingly to their half-life (A) and transcription rates (B), Pol II density (C) and gene length (D) sorted by the expression level in *ceg1-AA* (DMSO). ns=P > 0.05; *=P ≤ 0.05; **=P ≤ 0.01; ***= P ≤ 0.001; ****= P ≤ 0.0001.

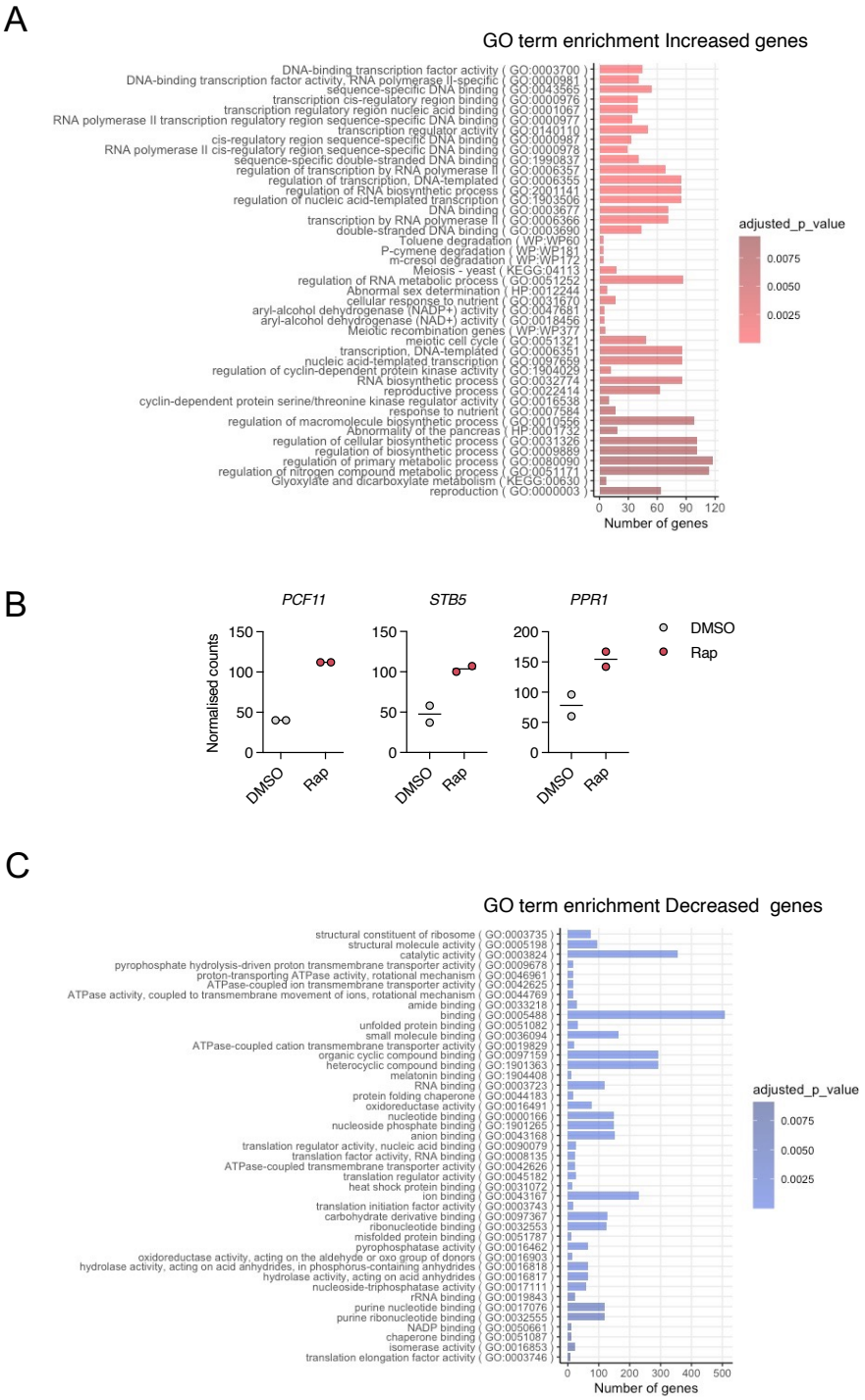

Figure S3.

A. GO terms associated with increased mRNAs in *ceg1-AA* (Rap). Charts showing the number of the genes belonging to the specific GO group. The classes are listed in a p-value increasing order. **B.** Plots showing the counts per gene for *PCF11*, *STB5* and *PPR1* obtained from the RNA-seq experiment. Charts showing the number of the genes belonging to the specific GO group. The classes are listed in a p-value increasing order. **C.** GO terms associated with decreased mRNAs in *ceg1-AA* (Rap). Charts

778 showing the number of the genes belonging to the specific GO group. The classes are listed in a p-
779 value increasing order.
780

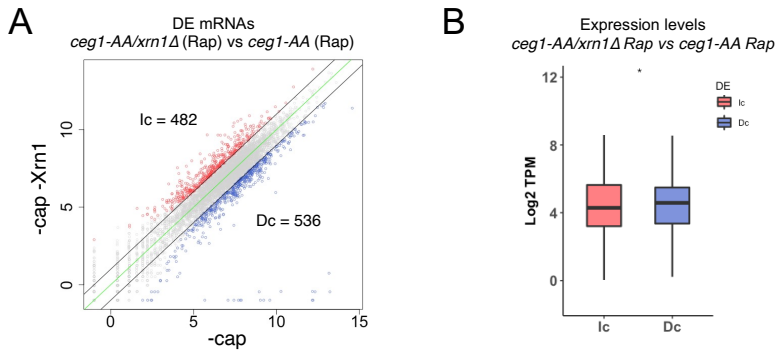

781
782 **Figure S4.**
783 **A.** RNA-seq analysis showing differential accumulation of mRNA species in *ceg1-AA/xrn1Δ* (Rap) strain
784 after 45 min of rapamycin treatment compared to *ceg1-AA* (Rap). Decreased (D) RNA species showing
785 log2 Fold change <1 are in blue. Increased (I) RNA species with log2 Fold change >1 are labelled in
786 red. The zero-change line is in green. **B.** Differentially expressed mRNAs in *ceg1-AA/xrn1Δ* (Rap) vs
787 *ceg1-AA* (Rap) sorted by their expression levels: Increased (I) or decreased (D). The expression levels
788 were calculated by Transcript Per Million (TPM) value in *ceg1-AA* (DMSO).
789

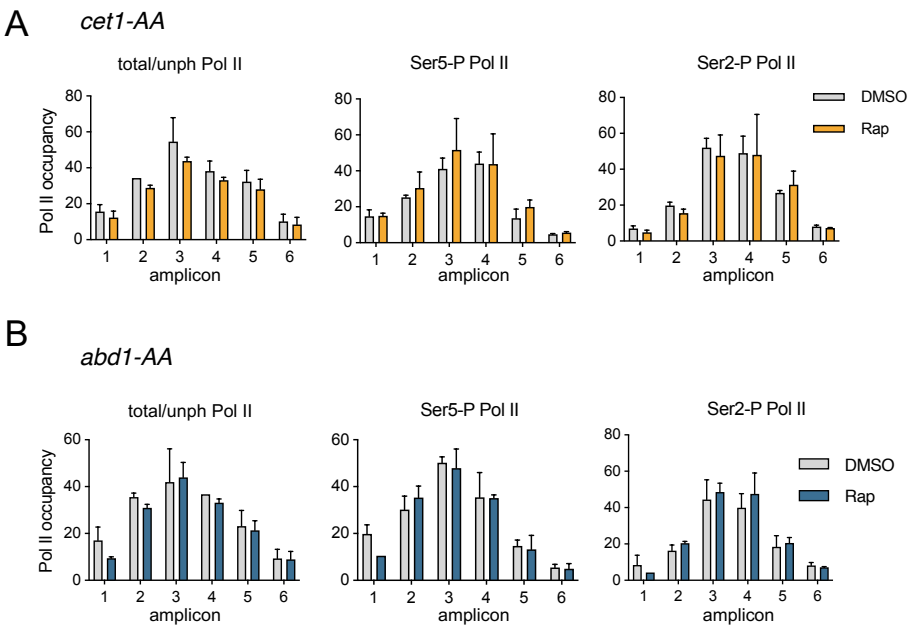

790

791 **Figure S5.**

792 **A-B.** The distribution of total/unphosphorylated (total/unph) Pol II as well as serine 5-phosphorylated
793 (Ser5-P) and serine 2-phosphorylated (Ser2-P) Pol II isoforms over *ADH1* in control (DMSO) and after
794 45 min of rapamycin (Rap) in (A) *cet1-AA* and *abd1-AA* strain (B). The location of the amplicons used
795 for the ChIP-qPCR is shown above the charts. The error bars show the standard deviation of three
796 independent ChIP-qPCR experiments.

797

798

799

800

801

802

803

804

805

806

807

808

809

810

811

812

813

814

815

816

817 **REFERENCES**

818 Akiyama, B. M., Eiler, D. and Kieft, J. S. (2017) 'Structured RNAs that evade or
819 confound exonucleases: function follows form', pp. 40–47. doi:
820 10.1016/j.sbi.2015.12.006.Structured.
821 Bartkowiak, B. and Greenleaf, A. L. (2011) 'Phosphorylation of RNAPII: To P-TEFB
822 or not to P-TEFB?', *Transcription*, 2(3), pp. 115–119. doi: 10.4161/trns.2.3.15004.
823 Bird, G. *et al.* (2005) 'Ribozyme cleavage reveals connections between mRNA
824 release from the site of transcription and pre-mRNA processing', *Molecular Cell*,
825 20(5), pp. 747–758. doi: 10.1016/j.molcel.2005.11.009.
826 Brannan, K. *et al.* (2012) 'mRNA Decapping Factors and the Exonuclease Xrn2
827 Function in Widespread Premature Termination of RNA Polymerase II Transcription',
828 *Molecular Cell*. Elsevier Inc., 46(3), pp. 311–324. doi: 10.1016/j.molcel.2012.03.006.
829 Chu, C. and Shatkin, A. J. (2008) 'Apoptosis and autophagy induction in mammalian
830 cells by small interfering RNA knockdown of mRNA capping enzymes.', *Molecular*
831 *and cellular biology*, 28(19), pp. 5829–5836. doi: 10.1128/MCB.00021-08.
832 Contreras, X., Benkirane, M. and Kiernan, R. (2013) 'Premature termination of
833 transcription by RNAP II: The beginning of the end', *Transcription*, 4(2). doi:
834 10.4161/trans.24148.
835 Cougot, N. *et al.* (2004) '"Cap-tabolism"', *Trends in Biochemical Sciences*, 29(8), pp.
836 436–444. doi: 10.1016/j.tibs.2004.06.008.
837 Decroly, E. *et al.* (2012) 'Conventional and unconventional mechanisms for capping
838 viral mRNA', *Nature Reviews Microbiology*. Nature Publishing Group, 10(1), pp. 51–
839 65. doi: 10.1038/nrmicro2675.
840 Dieci, G., Preti, M. and Montanini, B. (2009) 'Eukaryotic snoRNAs: A paradigm for
841 gene expression flexibility', *Genomics*, 94(2), pp. 83–88. doi:

842 https://doi.org/10.1016/j.ygeno.2009.05.002.
843 Doamekpor, S. K. *et al.* (2020) 'A novel 5′-hydroxyl dinucleotide hydrolase activity for
844 the DXO/Rai1 family of enzymes', *Nucleic Acids Research*. Oxford University Press,
845 48(1), pp. 349–358. doi: 10.1093/nar/gkz1107.
846 Dyer, N. P., Shahrezaei, V. and Hebenstreit, D. (2019) 'LiBiNorm: an htseq-count
847 analogue with improved normalisation of Smart-seq2 data and library preparation
848 diagnostics.', *PeerJ*, 7, p. e6222. doi: 10.7717/peerj.6222.
849 Eaton, J. D. *et al.* (2020) 'A unified allosteric / torpedo mechanism for transcriptional
850 termination on human protein-coding genes', pp. 1–14. doi:
851 10.1101/gad.332833.119.
852 Eaton, J. D. and West, S. (2020) 'Termination of Transcription by RNA Polymerase
853 II: BOOM!', *Trends in Genetics*. Elsevier Ltd, 36(9), pp. 664–675. doi:
854 10.1016/j.tig.2020.05.008.
855 Fortes, P. *et al.* (1999) 'Genetic and physical interactions involving the yeast nuclear
856 cap-binding complex.', *Molecular and cellular biology*, 19(10), pp. 6543–6553. doi:
857 10.1128/MCB.19.10.6543.
858 Furuichi, Y. (2015) 'Discovery of m 7 G-cap in eukaryotic mRNAs', *Proceedings of*
859 *the Japan Academy. Series B, Physical and biological sciences*, 91(8), pp. 394–409.
860 Gonatopoulos-Pournatzis, T. and Cowling, V. H. (2014) 'Cap-binding complex
861 (CBC)', *Biochemical Journal*, 457(2), pp. 231–242. doi: 10.1042/BJ20131214.
862 Grzechnik, P. *et al.* (2018) 'Nuclear fate of yeast snoRNA is determined by co-
863 transcriptional Rnt1 cleavage', *Nature Communications*. Springer US, 9(1). doi:
864 10.1038/s41467-018-04094-y.
865 Harlen, K. M. *et al.* (2016) 'Comprehensive RNA Polymerase II Interactomes Reveal
866 Distinct and Varied Roles for Each Phospho-CTD Residue', *Cell Reports*. The

867 Authors, 15(10), pp. 2147–2158. doi: 10.1016/j.celrep.2016.05.010.
868 Harlen, K. M. and Churchman, L. S. (2017) 'The code and beyond: Transcription
869 regulation by the RNA polymerase II carboxy-terminal domain', *Nature Reviews*
870 *Molecular Cell Biology*. Nature Publishing Group, 18(4), pp. 263–273. doi:
871 10.1038/nrm.2017.10.
872 Haruki, H., Nishikawa, J. and Laemmli, U. K. (2008) 'The Anchor-Away Technique:
873 Rapid, Conditional Establishment of Yeast Mutant Phenotypes', *Molecular Cell*,
874 31(6), pp. 925–932. doi: 10.1016/j.molcel.2008.07.020.
875 Hausmann, S., Pei, Y. and Shuman, S. (2003) 'Homodimeric quaternary structure is
876 required for the in vivo function and thermal stability of Saccharomyces cerevisiae
877 and Schizosaccharomyces pombe RNA triphosphatases', *Journal of Biological*
878 *Chemistry*, 278(33), pp. 30487–30496. doi: 10.1074/jbc.M303060200.
879 Hurowitz, E. H. and Brown, P. O. (2003) 'Genome-wide analysis of mRNA lengths in
880 Saccharomyces cerevisiae.', *Genome biology*, 5(1), p. R2. doi: 10.1186/gb-2003-5-
881 1-r2.
882 Izaurralde, E. *et al.* (1994) 'A nuclear cap binding protein complex involved in pre-
883 mRNA splicing.', *Cell*. United States, 78(4), pp. 657–668. doi: 10.1016/0092-
884 8674(94)90530-4.
885 Izaurralde, E. *et al.* (1995) 'A cap-binding protein complex mediating U snRNA
886 export.', *Nature*. England, 376(6542), pp. 709–712. doi: 10.1038/376709a0.
887 Jiao, X. *et al.* (2010) 'Identification of a quality-control mechanism for mRNA 5′-end
888 capping', *Nature*. Nature Publishing Group, 467(7315), pp. 608–611. doi:
889 10.1038/nature09338.
890 Jimeno-González, S. *et al.* (2010) 'The Yeast 5′-3′ Exonuclease Rat1p Functions
891 during Transcription Elongation by RNA Polymerase II', *Molecular Cell*, 37(4), pp.

892 580–587. doi: 10.1016/j.molcel.2010.01.019.
893 Jinek, M., Scott M. Coyle and Doudna, and J. A. (2014) ‘Coupled 5′ nucleotide
894 recognition and processivity in Xrn1- mediated mRNA decay’, *Bone*, 23(1), pp. 1–7.
895 doi: 10.1016/j.molcel.2011.02.004.Coupled.
896 Kim, M. *et al.* (2004) ‘The yeast Rat1 exonuclease promotes transcription termination
897 by RNA polymerase II’, *Nature*, 432(7016), pp. 517–522. doi: 10.1038/nature03041.
898 Lewis, J. D. and Izaurralde, E. (1997) ‘The role of the cap structure in RNA
899 processing and nuclear export’, *European Journal of Biochemistry*, 247(2), pp. 461–
900 469. doi: 10.1111/j.1432-1033.1997.00461.x.
901 Lidschreiber, M., Leike, K. and Cramer, P. (2013) ‘Cap Completion and C-Terminal
902 Repeat Domain Kinase Recruitment Underlie the Initiation-Elongation Transition of
903 RNA Polymerase II’, *Molecular and Cellular Biology*, 33(19), pp. 3805–3816. doi:
904 10.1128/MCB.00361-13.
905 Mao, X., Schwer, B. and Shuman, S. (1996) ‘Mutational analysis of the
906 Saccharomyces cerevisiae ABD1 gene: cap methyltransferase activity is essential
907 for cell growth’, *Molecular and Cellular Biology*, 16(2), pp. 475–480. doi:
908 10.1128/mcb.16.2.475.
909 Marquardt, S., Hazelbaker, D. Z. and Buratowski, S. (2011) ‘Distinct RNA
910 degradation pathways and 3’ extensions of yeast non-coding RNA species’,
911 *Transcription*, 2(3), pp. 145–154. doi: 10.4161/trns.2.3.16298.
912 Martinez-Rucobo, F. W. *et al.* (2015) ‘Molecular Basis of Transcription-Coupled Pre-
913 mRNA Capping’, *Molecular Cell*. Elsevier Inc., 58(6), pp. 1079–1089. doi:
914 10.1016/j.molcel.2015.04.004.
915 Pelechano, V., Wei, W. and Steinmetz, L. M. (2013) ‘Extensive transcriptional
916 heterogeneity revealed by isoform profiling’, *Nature*. doi: 10.1038/nature12121.

Perrotta, A. T., Shih, I. and Been, M. D. (1999) ‘Imidazole Rescue of a Cytosine Mutation in a Self-Cleaving Ribozyme’, *Science*. American Association for the Advancement of Science, 286(5437), pp. 123–126. doi: 10.1126/science.286.5437.123.

Ramanathan, A., Robb, G. B. and Chan, S. H. (2016) ‘mRNA capping: Biological functions and applications’, *Nucleic Acids Research*, 44(16), pp. 7511–7526. doi: 10.1093/nar/gkw551.

Schroeder, S. C. *et al.* (2000) ‘Dynamic association of capping enzymes with transcribing RNA polymerase II’, *Genes and Development*, 14(19), pp. 2435–2440. doi: 10.1101/gad.836300.

Schwer, B., Mao, X. and Shuman, S. (1998) ‘Accelerated mRNA decay in conditional mutants of yeast mRNA capping enzyme’, *Nucleic Acids Research*, 26(9), pp. 2050–2057. doi: 10.1093/nar/26.9.2050.

Shatkin, A. J. and Manley, J. L. (2000) ‘The ends of the affair: Capping and polyadenylation’, *Nature Structural Biology*, 7(10), pp. 838–842. doi: 10.1038/79583.

Topisirovic, I. *et al.* (2011) ‘Cap and cap-binding proteins in the control of gene expression’, *Wiley Interdisciplinary Reviews: RNA*, 2(2), pp. 277–298. doi: 10.1002/wrna.52.

Tsukamoto, T. *et al.* (1997) ‘Isolation and characterization of the yeast mRNA capping enzyme beta subunit gene encoding RNA 5’-triphosphatase, which is essential for cell viability.’, *Biochemical and biophysical research communications*. United States, 239(1), pp. 116–122. doi: 10.1006/bbrc.1997.7439.

Urrutia, A. O. and Hurst, L. D. (2003) ‘The signature of selection mediated by expression on human genes’, *Genome Research*, 13(10), pp. 2260–2264. doi: 10.1101/gr.641103.

942 Varshney, D. *et al.* (2018) ‘mRNA Cap Methyltransferase, RNMT-RAM, Promotes
943 RNA Pol II-Dependent Transcription’, *Cell Reports*. ElsevierCompany., 23(5), pp.
944 1530–1542. doi: 10.1016/j.celrep.2018.04.004.
945 West, S., Gromak, N. and Proudfoot, N. J. (2004) ‘Human 5′ → 3′ exonuclease Xm2
946 promotes transcription termination at co-transcriptional cleavage sites’, *Nature*,
947 432(7016), pp. 522–525. doi: 10.1038/nature03035.
948 Wyers, F. *et al.* (2005) ‘Cryptic Pol II transcripts are degraded by a nuclear quality
949 control pathway involving a new poly(A) polymerase’, *Cell*, 121(5), pp. 725–737. doi:
950 10.1016/j.cell.2005.04.030.
951 Xiang, S. *et al.* (2009) ‘Structure and function of the 5′3′ exoribonuclease Rat1 and
952 its activating partner Rai1’, *Nature*. Nature Publishing Group, 458(7239), pp. 784–
953 788. doi: 10.1038/nature07731.
954 Xu, Z. *et al.* (2009) ‘Bidirectional promoters generate pervasive transcription in
955 yeast’, *Nature*. doi: 10.1038/nature07728.
956
957
958